Bax activation blocks self-renewal and induces apoptosis of human glioblastoma stem cells

Simona Daniele[1], Deborah Pietrobono[1], Barbara Costa[1], Mariateresa Giustiniano[2], Valeria La Pietra[2], Chiara Giacomelli[1], Giuseppe La Regina[3], Romano Silvestri[3], Sabrina Taliani[1], Maria Letizia Trincavelli[1], Federico Da Settimo[1], Ettore Novellino[2], Claudia Martini[1*], Luciana Marinelli[2*].

[1]Department of Pharmacy, University of Pisa, Pisa, Italy.
[2]Department of Pharmacy, University of Naples Federico II, Napoli, Italy.
[3]Istituto Pasteur Italia - Fondazione Cenci Bolognetti, Dipartimento di Chimica e Tecnologie del Farmaco, Sapienza Università di Roma, Roma, Italy.

*Correspondence and requests for materials should be addressed to C.M and LM. Department of Pharmacy, University of Pisa, Via Bonanno 6, 56126 Pisa, Italy and Department of Pharmacy, University of Naples Federico II, Via D. Montesano 49, 80131 Napoli, Italy. E-mail addresses: claudia.martini@unipi.it and lmarinel@unina.it.

Abstract

Glioblastoma (GBM) is characterized by a poor response to conventional chemotherapeutic agents, attributed to the insurgence of drug resistance mechanisms and to the presence of a subpopulation of glioma stem cells (GSCs). GBM cells and GSCs present, among others, an overexpression of anti-apoptotic proteins and an inhibition of pro-apoptotic ones, which help to escape apoptosis. Among pro-apoptotic inducers, the Bcl-2 family protein Bax has been recently emerged as a promising new target in cancer therapy along with first BAX activators (BAM7, Compound 106 and SMBA1). Herein, a derivative of BAM-7, named BTC-8, was employed to explore the effects of Bax activation in different human GBM cells and in their stem cell subpopulation. BTC-8 inhibited GBM cell proliferation, arrested cell-cycle and induced apoptosis through the induction of mitochondrial membrane permeabilization. Most importantly, BTC-8 blocked proliferation and self-renewal of GSCs, and induced their apoptosis. Noteworthy, BTC-8 was demonstrated to sensitize both GBM cells and GSCs to the alkylating agent temozolomide. Overall, our findings shed light on the effects and on the relative molecular mechanisms related to Bax activation in GBM, and suggest Bax-targeting compounds as promising therapeutic tools against the GSC reservoir.

Key words: Bcl-2 family, Bax activation; glioblastoma; cancer stem cells; pro-apoptotic proteins.

Introduction

Glioblastoma (GBM) is a highly invasive and aggressive brain tumour[1]. Current standard of care includes surgical resection, radiation, and chemotherapy with the alkylating agent temozolomide (TMZ). More recently, dendritic cell vaccine, cytomegalovirus cytotoxic T lymphocytes and immune check point inhibitors such as nivolumab or pembrolizumab, have entered diverse phases of clinical trials for patients with recurrent GBM (https://www.clinicaltrial.gov). Nevertheless, at present, GBM has a very poor prognosis, with a 5-year survival rate of 4–5%[2], attributed to tumor location, heterogeneity of tumor formation and the occurrence of drug-resistance. Thus, today it is well-known that, similarly to other cancers, a stem cell-like population is responsible for GBM maintenance and proliferation[3-5]. Glioma cancer stem cells (GSCs) have been demonstrated to play a pivotal role in GBM genesis, as well as in its recurrences following treatment, suggesting that innovative stem cell-orientated therapies may be an effective strategy to significantly improve GBM treatment[6,7]. Unfortunately, several findings have shown that these cells are intrinsically more resistant to radiation and chemotherapy compared with non-cancer stem cells (CSCs)[8-10]. Similar findings have been found in a mouse model of GBM relapse[11]. Overall, these findings indicate that distinct or combined strategies to overcome GSC resistance[6] are urgently needed.

A huge amount of data indicates that GSCs display a prominent deregulation of apoptotic/survival pathways, which seems to contribute to their intrinsic chemo-resistance. This deregulation may result, among others, from alterations in mitochondrial proteins, providing alternative therapeutic opportunities to find novel chemotherapeutics[12]. In this respect, the mitochondrial Bcl-2 family proteins constitute, to date, one of the principal apoptosis regulators[13]. Within this family, three main subgroups are known: (i) the anti-apoptotic members (e.g., BCL-2, BCL-XL, MCL-1, A1), (ii) the pro-apoptotic members (e.g., Bak and Bax), and (iii) the pro-apoptotic BH3-only proteins (e.g., BID, BIM, PUMA, BAD, NOXA) [14-16].

Overexpression of pro-survival Bcl-2 family members has been documented in several human malignancies, including GBM[17,18], and related to chemoresistance and aggressive relapse[19,20]. Preclinical data have demonstrated that the pharmacological inhibition of such proteins can reactivate apoptosis and enhance the efficacy of conventional chemotherapies[17,21]. In immortalized glioma and GBM patient-derived GSC models, combined pharmacological interference of Bcl-2 family and other aberrantly active pro-survival pathways (e.g., PI3K signaling pathway or histone deacetylase) has been recently emerged as an effective strategy to overcome endogenous resistance to apoptosis[22,23].

Structure-aided medicinal chemistry have led to the development of several BH3 mimetic compounds[24,25]. Only recently, BAX-based virtual screening campaigns led to the identification of three small molecules as activator (BAM-7,[26] Compound 106[27] and SMBA1[28]). Lately, we embarked in a BAM-7 lead optimization program that led to the compound BTC-8[16], that displayed an EC_{50} of 700 nM, one order of magnitude lower than that measured for BAM-7 at least in HuH7 cells (Human Hepatoma cell line).

Herein, the effects of a Bax Targeting Compound (BTC-8), alone or in combination with the alkylating agent TMZ, were assessed in human GBM cells and in their stem cell subpopulation. BTC-8 was demonstrated to inhibit GBM cell proliferation through the induction of MOMP. Most importantly, the compound significantly blocked GSC proliferation and self-renewal and enhanced TMZ-elicited effects inducing a long-lasting arrest of GBM cells, as well as of GSCs, on which TMZ is poorly active. Overall, our findings shed light on the effects and the relative molecular mechanisms related to a Bax activation in GBM, and suggest Bax-targeting compounds as a promising therapeutic strategy to eliminate the GSC reservoir.

Results and Discussion

Experimental plan.

BTC-8[16] was utilized to explore the effects of Bax pharmacological activation in GBM. Indeed, experimental evidences have been reported demonstrating that BTC-8 is selective for Bax[16]. The compound ability to interact with the human recombinant Bax and activate its proapoptotic function in different tumor cell populations have been recently demonstrated[16]. Herein, BTC-8 cellular activity and molecular mechanisms were explored in human GBM cell lines expressing wild type Bax[29] and in the respective stem cell counterpart (GSCs). In order to compare the compound effects to those induced by a conventionally GBM chemotherapy drug, the DNA alkylating compound TMZ was tested in parallel experiments, alone or in combination with the Bax activator.

BTC-8 inhibits U87MG cell proliferation and potentiates TMZ-induced antiproliferative effects.

As a first step, to establish the optimal single dose of BTC-8 to be used in the next experiments, U87MG cells were treated with BTC-8 increasing concentrations (ranging from 1 nM to 50 μM) for 72 h. A dose-dependent inhibition of proliferation was observed in BTC-8-treated U87MG cells with respect to control (Fig. 1A), yielding an IC_{50} value of 711.7 ± 7.2 nM. The maximal percentage of inhibition was of 59.4 ± 3.8, comparable to that elicited by 50 μM TMZ[30] (Fig. 1C). Based on these findings, 500 nM BTC-8 was chosen as representative concentration in further experiments.

In order to confirm if BTC-8-elicited effects could be ascribed to Bax activation, cell proliferation experiments were repeated after Bax silencing by specific siRNA. The silencing efficacy was verified by both real time PCR and western blotting analyses (Suppl. Fig. 1A and B). Due to specific siRNA protocol, cell proliferation was tested after 48 h instead of 72 h. As shown in Fig. 1B, BTC-8 induced significantly lower anti-proliferative effects in Bax-silenced U87MG cells after 48 h of incubation, thus demonstrating that Bax activation is effectively involved in BTC-8 elicited effects. The abolishment of BTC-8-elicited activity was not evidenced at the highest compound concentration (i.e., 50 μM, Fig. 1B), thus suggesting that additional effects may occur at high compound concentration.

Consistent with our findings, targeting Bax with BH3 mimetics compounds has been shown to reactivate autophagic cell death in resistant glioma cells[31]. Similarly, Bax translocation, as an index of its activation, has been demonstrated to mediate cytotoxicity in different glioma cells,

including U87MG[32].

To assess whether U87MG cells could resume proliferation, at the end of the treatment period (72 h), the culture medium was replaced with fresh medium not containing the drug (Scheme in Fig. 1). As depicted in Figure 1C, U87MG did not recover their growth after 72 h of washout. These results suggest that BTC-8 is able to block completely the proliferation of U87MG cells.

To determine if Bax activation can potentiate the antiproliferative effect of the alkylating agent temozolomide (TMZ) in GBM cells, BTC-8 and TMZ were combined together. Challenging U87MG cells for 72 h with 50 μM TMZ plus 500 nM BTC-8 produced a synergic/additive effect on the reduction of cell proliferation (Fig. 1C). Consistent with our data, Bcl-2 inhibitors have been demonstrated to enhance TMZ action in U87MG cells[33].

Moreover, BTC-8 *plus* TMZ blocked the ability of cells to recover proliferation (Fig. 1C), whereas, TMZ-treated cells resumed proliferation after drug wash-out (Fig. 1C). These results suggested that the BTC-8-induced Bax activation prevents U87MG cells to recover the normal growth and enhances TMZ antiproliferative activity.

To dissect in deep if synergic or additive affects can occur in the presence of BTC-8 and TMZ, an isobolar analysis was performed[30,34,35]. The co-treatment of U87MG cells with the two tested BTC-8/TMZ ratio (1:12 and 1:50) produced an interaction index (γ) of 0,9 and 0,8, respectively (Fig. 1D and Suppl. Table 1). These results demonstrated that the combination of the two drugs raised additive antiproliferative effects in human U87MG cells.

BTC-8 induces apoptosis and cell cycle block of U87MG cells.

We then investigated whether the reduction in proliferating cells elicited by BTC-8 could be associated with apoptosis and/or cell cycle block.

As a first step, the number of living and dead cells were monitored by the use of the Trypan blue exclusion assay. Cell counting by Trypan blue evidenced that BTC-8 reduced the number of living cells (Fig. 2A) and, when used at micromolar concentration, slightly but significantly enhanced the quote of dead cells (Fig. 2A). In order to assess if the living cells were activating death programs, the possible loss of plasmatic membrane asymmetry was checked. After U87MG cell treatment with BTC-8 (500 nM, for 72 h), approximately 23% of cells with membrane integrity showed phosphatidylserine externalisation (Fig. 2B and Suppl. Fig. 2A), suggesting an apoptosis activation. Consistent with these results, Bax activation by BH3 mimetics has been demonstrated to induce effectively apoptosis in GBM cells, including U87MG[31].

As expected, TMZ alone induced a significant induction of cellular apoptosis/death; when the

alkylating agent was applied in combination with BTC-8, a significant enhancement of early- and late-stages of cellular apoptosis was observed (Fig. 2C and Suppl. Fig. 2B). These results confirmed that BTC-8 can sensitize GBM cells to the apoptotic action of TMZ.

Cell cycle analysis showed that U87MG cell treatment with 500 nM BTC-8 for 72 h induced cell cycle disturbance, arresting cell cycle in the G2/M phase. Similar effects were shown in the TMZ-treated samples (Fig. 2C and Suppl. Fig. 2B). When BTC-8 was used in combination with TMZ (500 nM+50 μM), the amount of cell debris did not allow the analysis of cell cycle phases (data not shown). Based on these results, cell cycle experiments were repeated maintaining the ratio between BTC-8 and/or TMZ, while decreasing their concentrations in U87MG cells (i.e., 10 nM BTC-8 and 10 μM TMZ). The combination of lower concentrations of the two compounds evidenced a higher arrest in the G2/M phase, with a highest degree with respect to single treated cells (Suppl. Fig. 3A and B).

BTC-8 dissipates mitochondrial membrane potential (Δψm) in U87MG cells but does not induce activation of caspase 3/7.

Since Bax-like proteins has been related to mitochondrial permeabilization[36], the effects of BTC-8 on GBM cell mitochondrial depolarization (Δψm) were assessed. To this purpose, mitochondria isolated from U87MG cells were incubated with 500 nM BTC-8 for 15 min and then Δψm was measured. The results showed that the compound markedly reduced JC-1 accumulation in mitochondria isolated from U87MG cells (Fig. 2D and Suppl. Fig. 2D), confirming collapse of Δψm after Bax activation. Similarly, BH3 mimetics have been demonstrate to trigger mitochondrial depolarization in anoxia-sensitive glioma cells[31].

The experiments were repeated in mitochondria isolated from U87MG cells previously incubated with BTC-8 and/or TMZ for 72 h. BTC-8 caused a significant depolarization of mitochondria membrane potential (Fig. 2E and Supplementary Fig. 2D), confirming that Bax activation can directly affect mitochondria functionality. In contrast, TMZ induced a modest reduction of JC-1 accumulation (Fig. 2E and Suppl. Fig. 2D). A strong mitochondrial depolarization was noticed in samples co-treated with BTC-8 and TMZ (Fig. 2E and Suppl. Fig. 2D), suggesting that the combination of a Bax activator and an alkylating agent can induce a more pronounced effects on mitochondria functionality.

Bax-like proteins (Bax, Bak, and potentially Bok) trigger mitochondrial permeabilization, which is required for the release of proapoptotic factors from mitochondria and for the activation of caspase-dependent and -independent cell death pathways[36,37]. However, challenging U87MG cells with 500 nM BTC-8 for 72 h did not reveal any significant activation

of caspase 3/7 (Fig. 2F and Suppl. Fig. 2E), thus suggesting that BTC-8 triggered cell death occurred in a caspase independent manner. Similar results were obtained with TMZ alone and in co-treated samples (Fig. 2F and Suppl. Fig. 2E). Nevertheless, higher concentrations of TMZ have been demonstrated to activate caspases in the same GBM cells upon 6 h of treatment[38]. Furthermore, it should be mentioned that BTC-8 itself has been shown to induce activation of caspase-3 following Bax translocation in NB4 leukemic cells[16]. Based on these data, it can be speculated that different mechanisms may occur following Bax activation in GBM cells. Consistent with this hypothesis, BH3 mimetics and Bcl-2 inhibitors have been demonstrated to induce a caspase-independent apoptosis and autophagy of GBM cells[31,33]. Moreover, caspase-3 has been shown not to be involved in cell death mediated by Bcl-2/Bcl-xL antisense oligonucleotides in U87MG cells[39], thus suggesting that the Bcl-2 family protein do not require caspases in these cells. Of note, GBM cells are sensitive to caspase-dependent apoptosis caused by different proapoptotic stimuli, indicating that these cells preserve the ability to induce caspases as death effectors[31].

BTC-8 differentially affects cell proliferation in distinct GBM cell lines.

In order to extend our observations on the therapeutically potential of a Bax activator in this type of tumor, selected experiments were also performed in additional GBM cell lines, considering the heterogeneity of these cells. In particular, U343MG, ANGM-CSS (presenting wild-type p53)[40,41] and T98G cells (presenting a mutated p53)[42] were selected.

As depicted in Figure 3A, BTC-8 lead to a significant and concentration-dependent inhibition of ANGM-CSS cell proliferation, showing an IC_{50} value of 495,5 ± 40,8 nM, similarly to what observed in U87MG cells. Conversely, a weak but significant inhibitory effect was obtained with TMZ (Fig. 3A), consistent with literature data[40,41,43,44]. The combination of BTC-8 and TMZ showed a significant greater effects with respect to single-treated cells (Fig. 3A), demonstrating that Bax activation can sensitise TMZ-poorly responding cells. Accordingly, Bak, a Bax protein analogue, has been identified recently as a key factor for TMZ-induced apoptosis in GBM: these findings may also account for the additive effects of a TMZ-BTC-8 treatment, and confirm the pro-apoptotic protein Bax as a promising target to overcome therapeutic resistance toward TMZ[45].

Challenging T98G cells with BTC-8 for 72 h did not significantly affect cell proliferation (Fig. 3C). As these cells present a mutated form of the tumor suppressor p53, such results may suggest that the pro-apoptotic effect of Bax activation requires a wild-type p53. In this respect, in a recent work Bcl-xL inhibitors have been shown to induce Bax full activation and the

subsequent cell death induction by the p53 pathway[46].

Surprisingly, although presenting a wild-type p53, U343MG cells were not affected by a 72 h treatment with high BTC-8 concentrations (Fig. 3B), suggesting that other factors than the p53 status may contribute to GBM cell sensitivity to Bax activation. Nevertheless the poor sensitivity of U343MG cells, the combination of BTC-8 and TMZ was still able to potentiate TMZ-induced effects (Fig. 3B). The comparable BTC-8-induced antitumoral effects observed in wild-type p53 U343MG (Fig. 3B) and p53-null T98G (Fig 3C) cells could be due to expression of p73 in this latter cell line.

Overall, such results confirmed that Bax activation sensitizes GBM cells to TMZ-elicited effects in GBM cells. Similarly, the pharmacological inhibition of the antiapoptotic proteins Bcl-2 has been demonstrated to improve TMZ action in different glioma cells, including U87MG and U343MG[33].

To explore the putative reasons at the basis of the different GBM cell responses to BTC-8, the mRNA levels of Bcl-2 family proteins was investigated in the different GBM cell lines, since a correlation between the expression of Bcl2-like proteins and pro-apoptotic effects has been demonstrated in primary GBM[24,39]. As depicted in Figure 3D, ANGM-CSS presented a significant lower mRNA content of the antiapoptotic members Bcl-2 and Bcl-XL with respect to U87MG cells. These results may account to the great ANGM-CSS response to Bax activation. Consistent with this hypothesis, the specific down-regulation of both Bcl-2 and Bcl-XL expression in GBM cell lines by antisense oligonucleotides results in spontaneous cell death[39].

Conversely, the p53-wild-type U343MG cells displayed a significant higher mRNA expression of Bcl-2 (Fig. 3D), which could contribute to their poor sensitivity to BTC-8. Based on literature data, Bcl-2 overexpression in these cells may block p53-mediated effects, inhibiting, in particular, its binding to target gene promoters that control the apoptotic response to DNA damage, as well as the endogenous transcriptomic changes subsequent to genotoxic stress[47].

Interestingly, T98G cells were found to have a lower mRNA expression of Bcl-2, Bcl-XL, and of Bax (Fig. 3D). Such results suggest that the p53/Bax axis plays the major role in controlling BTC-8 mediated effects.

Consistent with these data, the Bax/Bcl-2 ratio, a common parameter of apoptosis[48-50] presented the following order: ANGM-CSS>T98G>U343MG (Suppl. Fig. 4). Such results reflect the sensitivity of GBM cells to BTC-8, consistent with recent literature data reporting an increase of Bax/Bcl-2 ratio when antiproliferative/apoptotic effects occur[48-51]. However, additional experiments will be required to explore in deep the molecular mechanisms of Bax activation

in the different GBM cell lines.

BTC-8 decreases U87MG-derived GSC proliferation.

Several evidences have demonstrated that CSCs play a major role in drug resistance and disease recurrence and that the development of effective therapeutic strategies to eliminate GSCs is critical to improve GBM treatment outcomes[9,52].

Therefore, the effects of BTC-8 on GSCs isolated from GBM cells were evaluated. The formation of neurospheres in U87MG cell cultures *in vitro* was induced by a specific neural stem-cell (NSC) medium[6,43,53]. Consistent with literature data[6,43,53], the spheres obtained using U87MG cells (Suppl. Fig. 5A) included significantly higher levels of the stem cell markers CD133/Nestin$^+$ cells and a smaller percentage of GFAP$^+$ cells compared with the pool of whole U87MG cells (Suppl. Fig. 5B). Moreover, GSCs presented a greater ability to form spheres with respect to adherent U87MG cells (51.5% GSC, 10.1% U87MG, $p < 0.001$, Suppl. Fig. 5C), indicating that GSCs retain a clonogenic and self-renewal potential. Finally, GSCs were confirmed to exhibit a higher resistance to TMZ with respect to U87MG cells after 72 h of incubation (Suppl. Fig. 5D)[41]. All together, these data support the reliability of GSC isolation.

First, the effect of BTC-8 and/or TMZ was explored on GSC proliferation. As depicted in Figure 4A, BTC-8 induced a concentration-dependent inhibition of GSC proliferation, yielding an IC_{50} value of 8.8 ± 0.9 nM after 7 days of cell incubation. Based on these data, GSCs were challenged with 50 nM BCT-8 in further experiments.

Such results suggest a great sensitivity of GSCs to Bax activation. Similarly, the BH3 mimetic ABT-737 has been demonstrated to reduce GSC proliferation[54], confirming that the activation of the Bax pathway is able to target the stem cell subpopulation of GBM.

Neurospheres were found to present significant greater Bax mRNA levels with respect to U87MG cells (Fig. 4B), thus suggesting a putative explanation for GSC sensitivity to BTC-8. However, previous studies have reported that CD133+-GSCs express elevated levels of anti-apoptotic proteins Bcl-2 and Bcl-XL[55]. Based on such data, it can be speculated that Bax activation in GSCs is able to overcome Bcl-2/Bcl-XL overexpression, reducing in turn GSC proliferation.

TMZ alone significantly inhibited GSC proliferation (Fig. 4C), as previously demonstrated[9]; the treatment for 7 days with 50 μM TMZ plus 50 nM BTC-8 had a synergic/additive effect on the reduction of neurosphere's proliferation (Fig. 4C). Such data suggest that Bax activation can sensitise GSCs to TMZ-mediated cytotoxicity.

Next, we assessed whether BTC-8-treated cells could resume their growth after drug removal

(treatment scheme, Fig. 4). After U87MG-GSC challenging with the compound, and a wash-out period of 7 days, the percentages of proliferating cells did not significantly increase, suggesting their overall inability to recover normal growth (Fig. 4C). TMZ-treated samples showed a trend toward growth re-starting after 72 h of cell wash-out, whereas challenging GSCs with both TMZ and BTC-8 triggered a long-lasting inhibition of GSC growth (Fig. 4C, 85.9 ± 3.6 % of inhibition, which persisted after 72 h of wash-out).

BTC-8 inhibits U87MG-derived GSC formation and induces apoptosis/cell cycle block.

A morphological analysis was performed in order to confirm the effects elicited by BTC-8, alone or in combination with TMZ, on GSCs isolated from U87MG cells. The results showed that 50 nM BTC-8 mediated inhibition of cell proliferation was accompanied by a reduction in the number (Fig. 5A and B) and in the area (Fig. 5A and C) occupied by GSCs in culture. Similar results were obtained challenging GSCs with TMZ for seven days (Fig. 5A-C). When combined together, the two drugs elicited significant greater effects on the reduction of number and area occupied by neurospheres (Fig. 5A-C) with respect to single-treated cells. These results confirmed that the co-treatment with a Bax activator and TMZ could represent a great strategy to block GSC proliferation.

The ability of BTC-8 to affect the formation of GSCs was then examined. To this purpose, adherent U87MG cells were switched to a defined serum-free NSC medium, and the cells were allowed to growth for nine days in the presence or absence of BTC-8 and/or TMZ (Fig. 5D, E and F). BTC-8 and TMZ decreased the diameter of the new formed spheres, suggesting their ability to inhibit the proliferation of *de novo* GSCs (Fig. 5E). Moreover, the compounds caused a reduction in the sphere number, indicating their capacity to alter the stem cell-generating ability of the GBM cells, too (Fig. 5F). Additive effects were noticed in the presence of a co-treatment with BTC-8/TMZ (Fig. 5D, E and F).

Cell cycle analysis demonstrated that challenging GSCs for 7 days with BTC-8, as well as with TMZ, induced cell cycle arrest in G2/M phase decreasing significantly the G0/G1 subpopulation (Fig. 6A and Suppl. Fig. 6A). As in U87MG cells, when BTC-8 was applied with TMZ, the amount of cell debris did not allow analysing cell cycle phases (data not shown). Treating GSCs with BTC-8 for 7 days caused a significant phosphatidylserine externalization in the presence of 7-AAD binding to DNA, thus denoting the induction of early and late apoptosis (Fig. 6B and Suppl. Fig. 6B). Consistent with our findings, Bax upregulation and Bcl-2 downregulation have been found to induce apoptosis of breast or cervical CSC [56,57].

Overall, these results demonstrated that the block of GSC proliferation was accompanied by

the induction of GSC apoptosis and by GSC cycle block.

BTC-8 dissipates mitochondrial membrane potential (Δψm) in U87MG-derived GSCs but does not induce activation of caspase 3/7.

The effects of BTC-8 on mitochondrial depolarization were assessed also in GSCs. GSCs were treated with the compound for 7 days, and then Δψm was measured in isolated mitochondria. The results showed that 50 nM BTC-8 markedly reduced JC-1 accumulation in mitochondria isolated from GSCs (Fig. 6C and Suppl. Fig. 6C). When combined with TMZ, an almost complete dissipation of mitochondrial membrane potential was evidenced (Fig. 6C and Suppl. Fig. 6C). Consistent with the data obtained in U87MG cells, BTC-8 alone or in combination with TMZ did not induce caspase 3/7 activation in GSCs (Fig. 6D and Suppl. Fig. 6D).

BTC-8 modulates the transcription of hypoxia-inducible factors in U87MG cells and in U87MG-derived GSCs.

Several studies have demonstrated that GBM cells, and in particular GSCs, are maintained within hypoxic niches and that hypoxia-inducible factors (HIFs), including HIF-1α and HIF-2α, play a key role in maintaining the stemness of these cells[53,58,59]. Therefore, the modulation of the HIF-1α transcript levels upon incubation with BTC-8 was investigated.

Challenging U87MG cells with 500 nM BTC-8 significantly decreased mRNA levels of HIF-1α and enhanced mRNA levels of HIF-2α (Fig. 7A), thus suggesting that the compound-elicited cytotoxic effects involve HIF modulation. Consistent with this hypothesis, silencing the HIF-1α gene resulted in the inhibition of GBM tumour growth[53,60]. The increase in HIF-2α mRNA elicited by BTC-8 and TMZ may represent a positive event, since in glioma cells HIF-2α has been demonstrated to repress the transcription of essential elements for cellular immortalization and transformation[61].

TMZ alone showed similar effects on the modulation of HIF-1α and HIF-2α (Fig. 7A). When applied with BTC-8, a further reduction in HIF-1α levels was noticed (Fig. 7A), thus suggesting that the compound can cooperate with TMZ in blocking HIF-1α signalling in GBM cells.

Similar experiments were repeated in GSCs (Fig. 7B). Neurospheres were confirmed to exhibit a higher increased expression of HIF-1α compared to the differentiated GBM cells (Fig. 7C), consistent with previously reported data[53,62,63]. BTC-8 did not induce any significant changes in HIF-1α level after 7 days of treatment (Fig. 7B). Similar effects were observed with TMZ alone (Fig. 7B). In contrast, BTC-8 and TMZ used alone significantly enhanced HIF-2α mRNA

levels (Fig. 7B). When the two drugs were combined together, a further increase in HIF-2α was evidenced (Fig. 7B).

HIF-2α has been shown to play a significant role in preserving cells an undifferentiated state[58,64]*;* nevertheless, the enhancement in the HIF-2α mRNA levels that was observed on the 7th day may be associated with effects on other signaling pathways. For example, such increase may block Notch, thus inhibiting cell proliferation, as supposed in previous papers[6,65].

BTC-8 differentially affects GSC proliferation in distinct GBM cell lines.

Proliferation experiments were performed in GSCs isolated from U343MG, ANGM-CSS and T98G cells. Consistent with the results obtained in the respective differentiated cells (see Fig. 3A), BTC-8 effectively inhibited ANGM-CSS-derived GSC proliferation (Fig. 8A), exhibiting greater antitumoral effects with respect to TMZ (Fig. 5A). When combined together, the two compounds induced a significant higher reduction of GSC proliferation with respect to single-treated cells (Fig. 8A). Challenging U343MG-deived GSCs with BTC-8 for 7 days significantly affected cell proliferation only at the highest tested concentration (Fig. 8B), thus confirming this GBM cell line as poorly-responder to Bax activation. In the presence of TMZ, a slight but significant enhancement of Bax-mediated effects were noticed (Fig. 8B). Overall, these data demonstrate the ability of BTC-8 to potentiate TMZ-elicited effects in GSCs isolated from different GBM cell lines.

Conversely, GSCs isolated from T98G cells did not respond to BTC-8 (Fig. 8C). TMZ showed a modest reduction of such neurospheres (Fig. 8C); in this case, the combination of TMZ plus BTC-8 was not able to induce additive effects (Fig. 8C), demonstrating that a functional p53 pathway is essential in GSCs as well. Accordingly, several evidences have identified p53 as one of the key regulation of normal and malignant stem/progenitor cell differentiation, self-renewal and tumorigenic potential[66].

BTC-8 does not affect viability/proliferation of normal human cell models. BTC-8 has previously found not to affect viability of normal cells[16]. Herein, in order to investigate further BTC-8 potential toxicity profile, both human mesenchymal stem cells (MSCs) and human lymphocytes were used as normal cell models. Challenging MSCs with the compound (1-100 μM) for 72 h did not significantly affect cell proliferation (Fig. 8D).

Human lymphocytes were confirmed to express Bax (Suppl. Fig. 7). In these cells, BTC-8, alone or in combination with TMZ, did not show any significant effect in the MTS assay (Fig. 8D). These data suggest that BTC-8 mechanism of action is directed preferentially toward

tumor cells.

Conclusions

GBM is characterized by a high rate of drug resistance and recurrence, due, at least in part, to the tumor ability to escape apoptosis and to the presence of a highly proliferative stem cell component. GBM cells and GSCs present, among others, an overexpression of anti-apoptotic proteins and an inhibition of proapoptotic ones. Among proapoptotic inducers, the Bcl-2 family protein Bax has been emerging as a promising new target in cancer. In the present paper, the Bax activator BTC-8 was provided to induce anti-proliferative effects, apoptosis and cell cycle block in human U87MG cells and in their stem cell counterpart, through the induction of mitochondrial membrane permeabilization. In particular, the compound inhibited cell proliferation with an IC_{50} value of 8.8 nM in U87MG-derived GSCs.

Importantly, BTC-8 was provided to potentate the chemotherapeutic action of TMZ, both in GBM cells and in GSCs. Considering that this alkylating agent, together with radiotherapy and surgery, is the international standard-of-care for thousands of people with GBM, the discovery of a new substance able to sensitize cells to TMZ may represent a starting point for the development of novel therapeutic strategies in this type of tumor.

Materials and methods

GBM cell-lines and GSC isolation. U87MG, U343MG, SH-SY5Y and T98G were obtained from the National Institute for Cancer Research of Genoa (Italy), American Type Culture Collection (USA) and Cell Lines Service GmbH (Germany), respectively. ANGM-CSS cells were kindly gifted by IRCCS Casa Sollievo della Sofferenza Hospital, Italy. Each cell line was monitored for DNA profiling and cultured as described[30,41].

To isolate GSCs from each GBM cell line, approximately 2.5 x 10^6 cells were suspended NSC medium as described[6,53]. The method accuracy for GSC isolation was verified in previous experiments[6,53] and further confirmed by Real Time RT-PCR analysis of stem cell (CD133, Nestin) and glial (GFAP) markers (see Supplementary Information). Furthermore, GSC clonogenic potential was verified by a limiting dilution initiation analysis[43], quantifying the "frequency of neurospheres initiation cells". Neurospheres or adherent U87MG cells were dissociated and seeded in NSC medium (1, 5, 10, 50, or 100 cells/well)[43]. The formed neurospheres were scored after 15 days using ELDA's online algorithm (http://bioinf.wehi.edu.au/software/ elda/).

Cell proliferation assays of GBM cells and GSCs. The human GBM cells (U87MG, U343MG, ANGM-CSS or T98G cells), neuroblastoma cells (SH-SY5Y), or GSCs were treated for the indicated times with fresh growth medium containing different concentrations of BTC-8, synthesized as previously described[16]. For the long-term treatment of cells, NSC or complete medium containing drugs was replaced every three days. When indicated, U87MG cells were treated with BTC-8 500 nM and TMZ 50 μM, alone or in combination. For wash-out experiments, U87MG cells or GSCs were treated with BTC-8 and/or TMZ for 72 h (U87MG cells) or 7 days (GSCs). At the end of treatments, medium-containing drugs was replaced by fresh medium, and cells were allowed to growth for the indicated days (3 days for GBM cells, 7 days for GSCs). At the end of treatments, cell proliferation was determined using the MTS assay, as described[43].

Isobolar analysis. A graphical assessment of BTC-8/TMZ synergy with regard to U87MG growth inhibition was performed using isobolographic analysis[30,34,35]. The IC_{50} of TMZ was plotted on the abscissa, and the iso-effective dose of BTC-8 was plotted on the ordinate. The theoretical additive effect of the two drugs is represented by the straight line connecting the two points. To determine whether the interaction between the two drugs was synergistic,

additive or antagonistic, the theoretical additive $IC_{50,add}$ was estimated from the dose-response curves of each drug administered individually. The interaction index, denoted by γ, is an assessment of the degree of synergism or antagonism. The index is defined by the isobolar relationship as follows[34,35]: $\gamma = a/A + b/B$ where A and B are the doses of drug A (alone) and B (alone) that give the specified effect, and (a,b) are the combination doses that produce the same effect[30].

siRNA mediated inhibition of Bax gene expression. Bax siRNA (Santa Cruz Biotecnology, Heidelberg, Germany) or siRNA scrambled was transfected to a final concentration of 100 nM, following the manufacturer's protocol[30]. The silence efficacy was verified by both real time PCR western blotting analyses (see below). 24 h after transfection, U87MG cells were incubated with different BTC-8 concentrations for 48 h, and cell proliferation was assessed as reported above.

Mitochondrial membrane potential dissipation analysis. The Δψm dissipation was assessed using the fluorescent dye 5,59,6,69-tetrachloro1,19,3,39-tetraethylbenzimidazolylcarbocyanine iodide (JC-1)[68]. U87MG or GSCs were treated with DMSO (control), or BTC-8 and/or TMZ for 72 h or 7 days, respectively. At the end of treatments, mitochondria were isolated from U87MG cells and GSCs using the Mitochondria Isolation Kit (Sigma Aldrich, Milan, Italy) following manufacturer's instructions. When indicated, isolated mitochondria were incubated directly with BTC-8 and/or TMZ for 15 min. Following the treatment period, 90 µl of the JWS and 10 µl (5 µg of proteins) of isolated mitochondria were added. Sample fluorescence (relative fluorescence units, RFU) was read in a fluorimeter (excitation wavelength at 490 nm and emission wavelength at 590 nm)[68].

RNA extraction and Real Time PCR analysis in U87MG cells and in GSCs. U87MG cells or GSCs were incubated with BTC-8 and/or TMZ for 72 h or 7 days, respectively. At the end of treatments, cells were collected, and total RNA was extracted using Rneasy® Mini Kit (Qiagen, Hilden, Germany). cDNA synthesis was performed with 500 ng of RNA (BioRad, Hercules, USA). RT-PCR reactions were prepared as reported. The nucleotide sequences, annealing temperature and product size of the primers have been previously reported[6,30,53]. PCR analyses using specific primer for Bax[30] was used to verify the efficacy of siRNA protocol.

Cell cycle analysis in GSCs. U87MG or GSCs were treated with DMSO, BTC-8 (10 nM, 50 nM or 500 nM) and/or TMZ (10 μM or 50 μM) for 72 h or 7 days, respectively. The measurement of the percentage of cells in the different cell phases was performed using the Muse™ Cell Analyzer (Merck KGaA, Darmstadt, Germany) as described previously[53,68].

Cellular apoptosis in U87MG cells and in GSCs. U87MG cells or GSCs were treated with DMSO (control), BTC-8 and/or TMZ for 72 h or 7 days, respectively. Living, apoptotic and dead cells were acquired and analyzed by Muse™ Cell Analyzer as described previously[53,68].

Caspase 3/7 activation. U87MG cells or GSCs were treated with BTC-8 (50 nM or 500 nM) and/or TMZ (50 μM) for 72 h or 7 days, respectively. Following treatment, cells with activated caspase 3/7 were acquired and analyzed by Muse™ Cell Analyzer following the manufacture's protocol.

Neurosphere formation assay. The ability of cells of monolayer cultures to initiate neurosphere formation were assessed by harvesting, washing, and resuspending monolayer cells in serum-free NSC medium. Cells were seeded into 96-well at 2 x 10^4 cells/well and incubated with DMSO (0.5%, control), or BTC-8 (50 nM), alone or in combination with TMZ (50 μM) for 9 days without disturbing the plates and without replenishing the medium. The number and the diameter of the new formed neurosphere were counted using the Image J program (version 1.41; Bethesda, MD, USA)[53].

Quantitation of the occupied area and the cellular processes of neurospheres. GSCs were plated in complete growth medium (day 0) and treated for seven days with BTC-8 (50 nM), alone or in combination with TMZ (50 μM). At the end of the treatment periods, the drug-containing media were replaced with fresh NSC medium, and the GSCs were allowed to grow for another 7 or 14 days. At the end of the treatment period, images were captured (15 images for each well), and the area occupied by neurospheres that had formed, as well as the length of cellular processes were quantified as described[6,53].

Isolation and culture of human MSCs and T lymphocytes. Human MSCs (Lonza, Milan, Italy),

were cultured in the specific growth medium, and maintained at 37°C in 5% CO_2. Mononuclear cell isolation was performed as previously reported[30]. MSCs (5 x 10^3 cells/well) or lymphocytes were seeded and incubated for 72 h with the indicated concentrations of BTC-8 and/or TMZ. At the end of treatments, the compound toxicity was verified using the MTS assay, as described above.

Western blotting analysis. siRNA-treated cells or human lymphocytes were collected and lysed[30]. Cell extracts were resolved in 7.5% SDS-PAGE, using a specific antibody for Bax (B8429, Sigma-Aldrich, Milan, Italy). GAPDH (Glyceraldehyde-3-Phosphate Dehydrogenase, G9545, Sigma-Aldrich, Milan, Italy) was employed as the loading control. The ImageJ Software was used to perform the densitometric analysis of immunoreactive bands (ACS Chem Neurosci. 2017 Jan 18;8(1):100-114).

Statistical analysis. Graph-Pad Prism (GraphPad Software Inc., San Diego, CA) was used for data analysis and graphic presentations. All data are presented as the mean ± SEM. One-way analysis of variance (ANOVA) with Bonferroni's corrected t-test for post-hoc pair-wise comparisons was used to perform statistical analysis[6,53].

Supporting information

Silence efficiency of Bax; index of isobolar analysis; plots of cell cycle, apoptotis, mitochondrial membrane potential dissipation, and caspase 3/7 assays in GBM cells and in GSCs; characterization of GSCs derived from GBM cells.

ABBREVIATIONS

GBM, Glioblastoma Multiforme

GSCs, Glioblastoma cancer stem cells

JC-1, 5,59,6,69-tetrachloro1,19,3,39-tetraethylbenzimidazolylcarbocyanine iodide

MSCs, mesenchymal stem cells

TMZ, temozolomide.

Author Contributions

S.D., D.P. and C.G. performed biological experiments; S.D., B.C. and M.L.T. analyzed the data and wrote the manuscript. V.L.P. and M.G. synthesized the compound and helped in writing the manuscript too. M.L.T, G.L.R., S.T., F.D.S., E.N and L.M. designed the study and played a key role as project supervisor. R.S., L.M. and C.M coordinated the project. All the authors contributed to and approved the final manuscript.

Funding sources

The study was supported by PRIN2015FCHJ8E.

Conflict of Interest

The authors declare no competing financial interest.

Figures

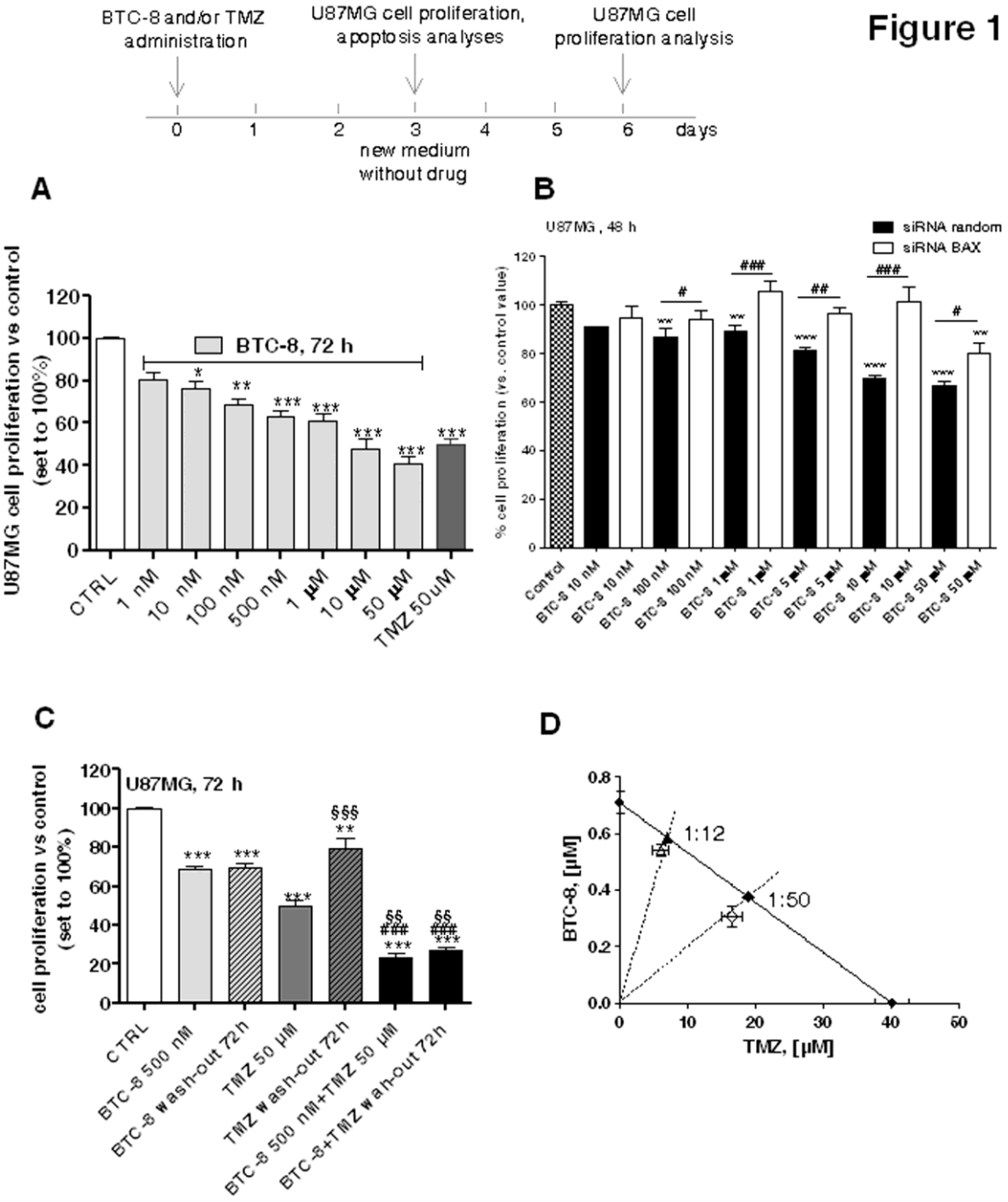
Figure 1
BTC-8 and/or TMZ administration
U87MG cell proliferation, apoptosis analyses
U87MG cell proliferation analysis
0 1 2 3 4 5 6 days
new medium without drug
A
U87MG cell proliferation vs control (set to 100%)
BTC-8, 72 h
CTRL
1 nM
10 nM
100 nM
500 nM
1 µM
10 µM
50 µM
TMZ 50uM
B
U87MG, 48 h
siRNA random
siRNA BAX
% cell proliferation (vs. control value)
Control
BTC-8 10 nM
BTC-8 10 nM
BTC-8 100 nM
BTC-8 100 nM
BTC-8 1 µM
BTC-8 1 µM
BTC-8 5 µM
BTC-8 5 µM
BTC-8 10 µM
BTC-8 10 µM
BTC-8 50 µM
BTC-8 50 µM
C
U87MG, 72 h
cell proliferation vs control (set to 100%)
CTRL
BTC-8 500 nM
BTC-8 wash-out 72h
TMZ 50 µM
TMZ wash-out 72h
BTC-8 500 nM+TMZ 50 µM
BTC-8+TMZ wash-out 72h
D
BTC-8, [µM]
TMZ, [µM]
1:12
1:50

Figure 2

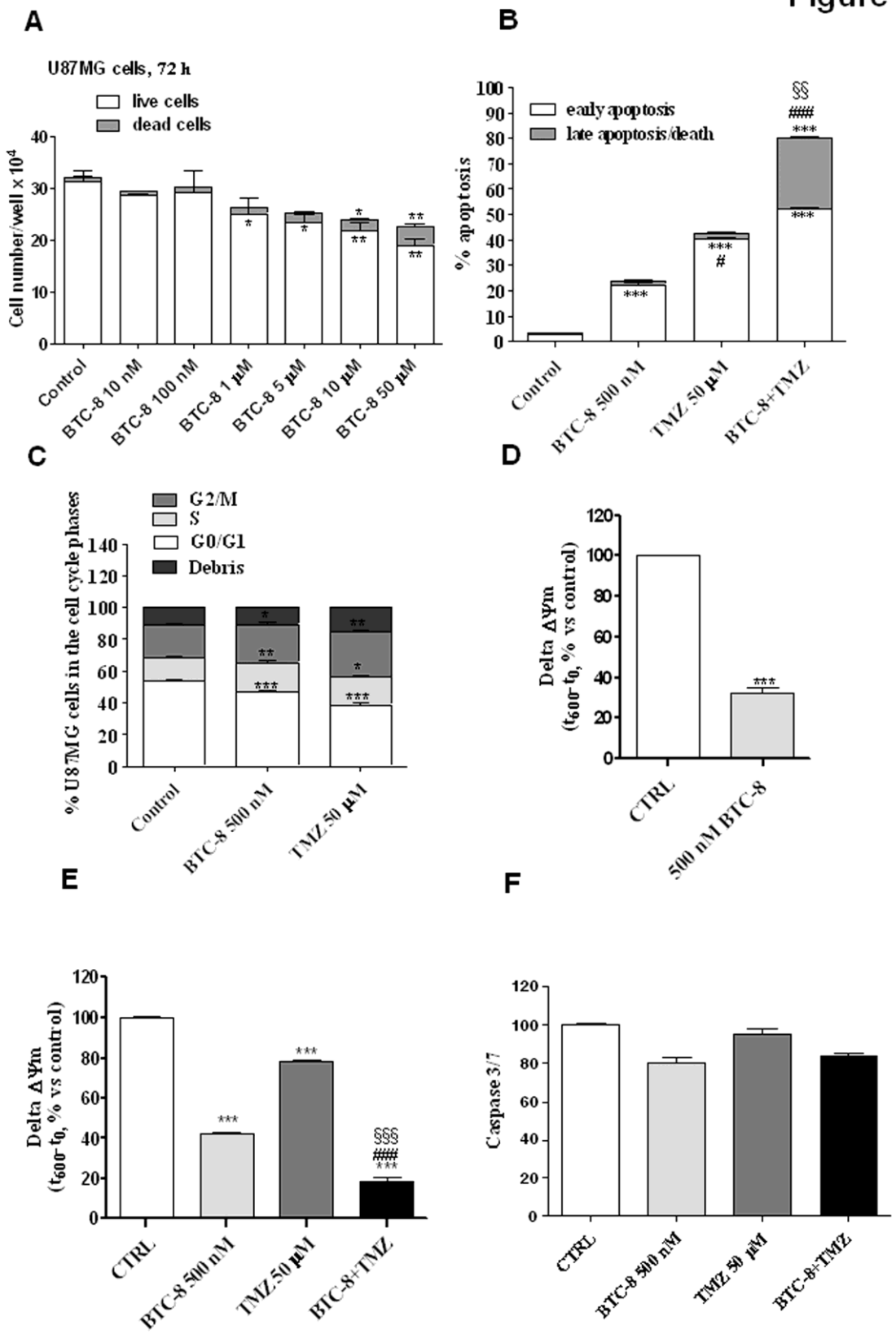
A
U87MG cells, 72 h
live cells
dead cells
Cell number/well x 10^4
Control
BTC-8 10 nM
BTC-8 100 nM
BTC-8 1 µM
BTC-8 5 µM
BTC-8 10 µM
BTC-8 50 µM
B
early apoptosis
late apoptosis/death
% apoptosis
Control
BTC-8 500 nM
TMZ 50 µM
BTC-8+TMZ
C
G2/M
S
G0/G1
Debris
% U87MG cells in the cell cycle phases
Control
BTC-8 500 nM
TMZ 50 µM
D
Delta ΔΨm
(t600-t0, % vs control)
CTRL
500 nM BTC-8
E
Delta ΔΨm
(t600-t0, % vs control)
CTRL
BTC-8 500 nM
TMZ 50 µM
BTC-8+TMZ
F
Caspase 3/7
CTRL
BTC-8 500 nM
TMZ 50 µM
BTC-8+TMZ

Figure 3

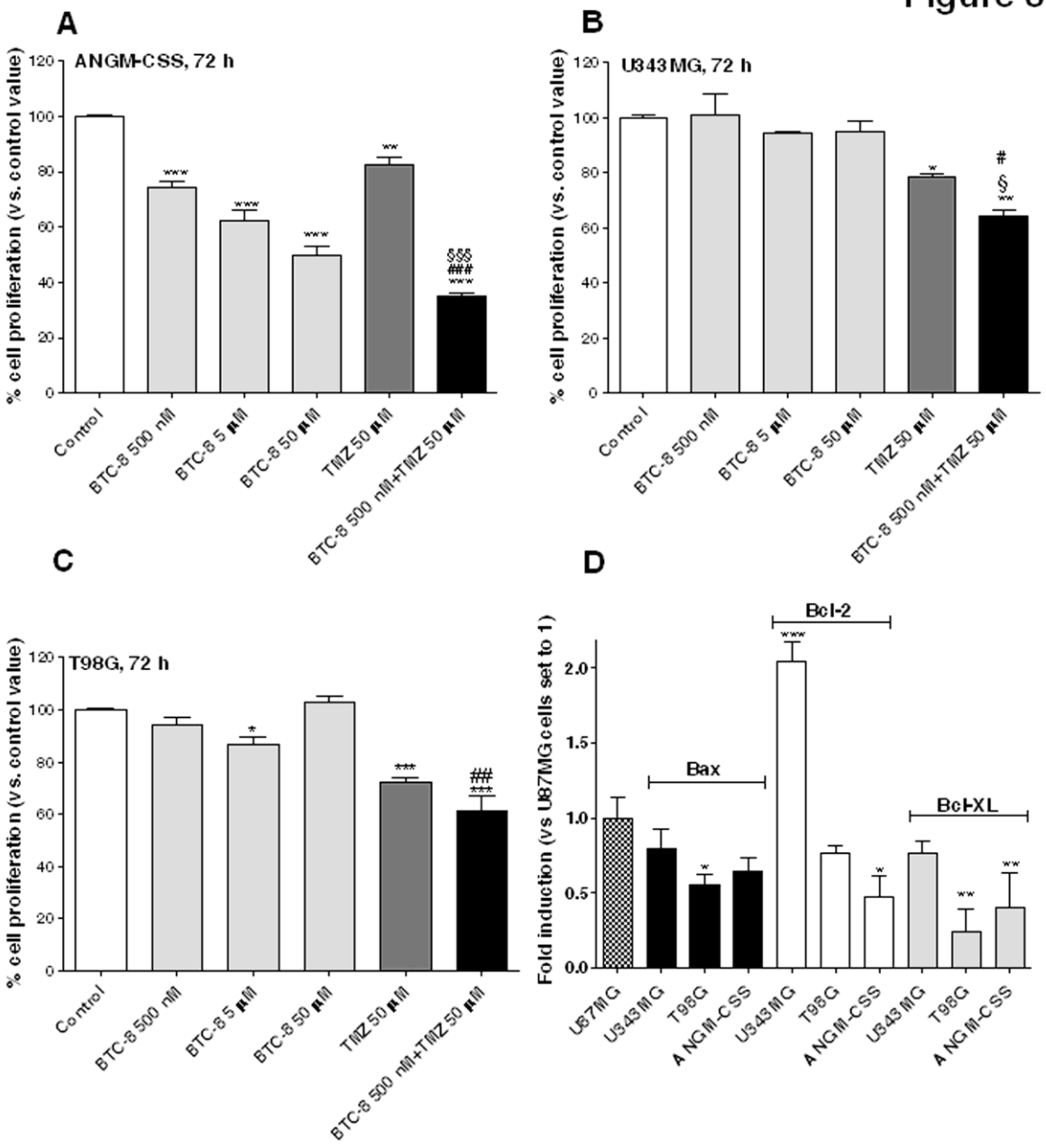
A
ANGM-CSS, 72 h
% cell proliferation (vs. control value)
Control
BTC-8 500 nM
BTC-8 5 pM
BTC-8 50 pM
TMZ 50 µM
BTC-8 500 nM+TMZ 50 µM
B
U343MG, 72 h
C
T98G, 72 h
D
Fold induction (vs U87MG cells set to 1)
Bax
Bcl-2
Bcl-XL
U87MG
U343MG
T98G
ANGM-CSS

Figure 4

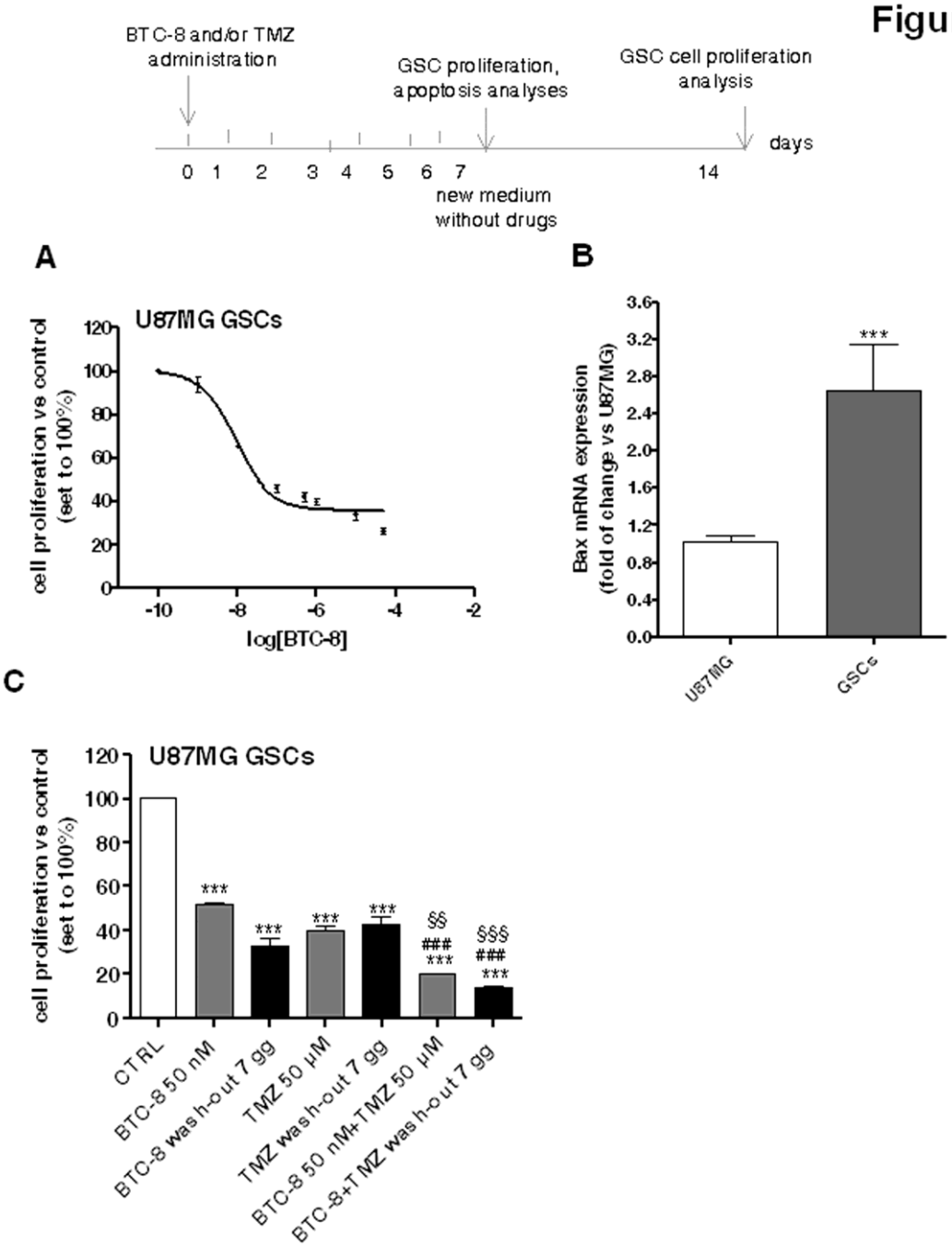
BTC-8 and/or TMZ administration
GSC proliferation, apoptosis analyses
GSC cell proliferation analysis
days
0 1 2 3 4 5 6 7
14
new medium without drugs
A
U87MG GSCs
cell proliferation vs control (set to 100%)
log[BTC-8]
B
Bax mRNA expression (fold of change vs U87MG)
U87MG
GSCs
C
U87MG GSCs
cell proliferation vs control (set to 100%)
CTRL
BTC-8 50 nM
BTC-8 wash-out 7 gg
TMZ 50 µM
TMZ wash-out 7 gg
BTC-8 50 nM+TMZ 50 µM
BTC-8+TMZ wash-out 7 gg

Figure 5

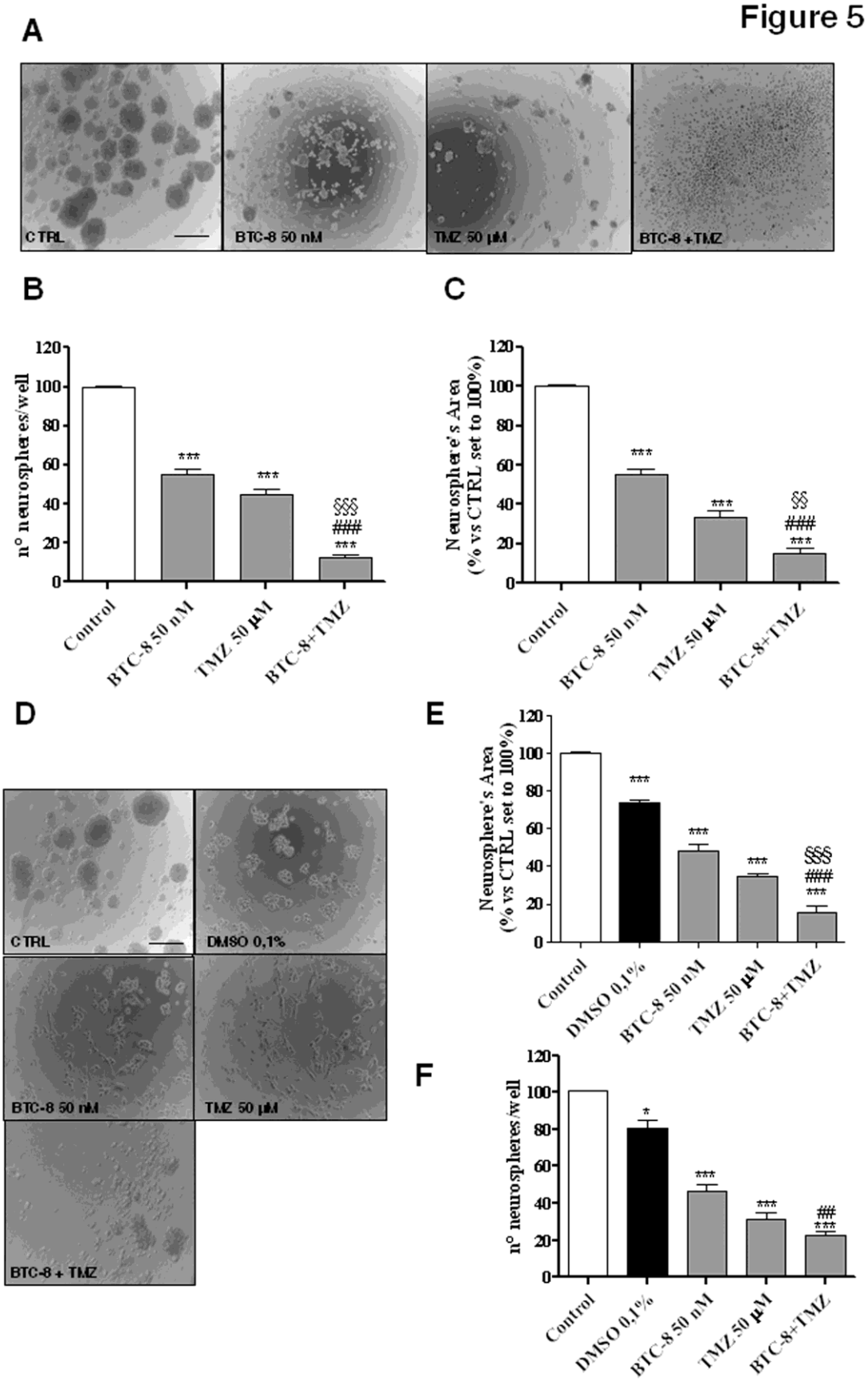
A
CTRL
BTC-8 50 nM
TMZ 50 µM
BTC-8 +TMZ
B
n° neurospheres/well
Control
BTC-8 50 nM
TMZ 50 µM
BTC-8+TMZ
C
Neurosphere's Area
(% vs CTRL set to 100%)
D
DMSO 0,1%
E
F

Figure 6

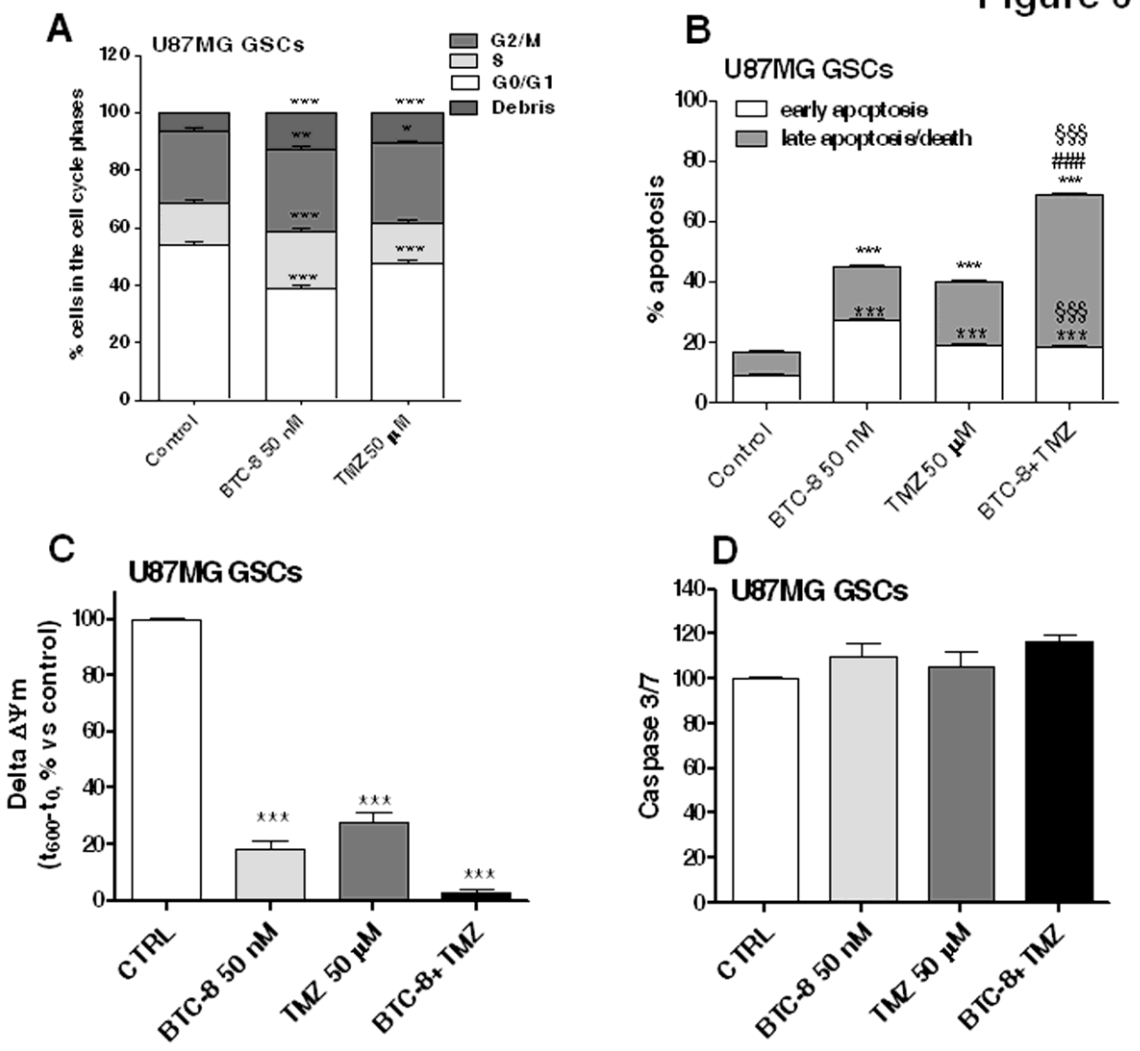
A
U87MG GSCs
G2/M
S
G0/G1
Debris
% cells in the cell cycle phases
Control
BTC-8 50 nM
TMZ 50 µM
B
U87MG GSCs
early apoptosis
late apoptosis/death
% apoptosis
Control
BTC-8 50 nM
TMZ 50 µM
BTC-8+TMZ
C
U87MG GSCs
Delta ΔΨm
(t600-t0, % vs control)
CTRL
BTC-8 50 nM
TMZ 50 µM
BTC-8+TMZ
D
U87MG GSCs
Caspase 3/7
CTRL
BTC-8 50 nM
TMZ 50 µM
BTC-8+TMZ

Figure 7

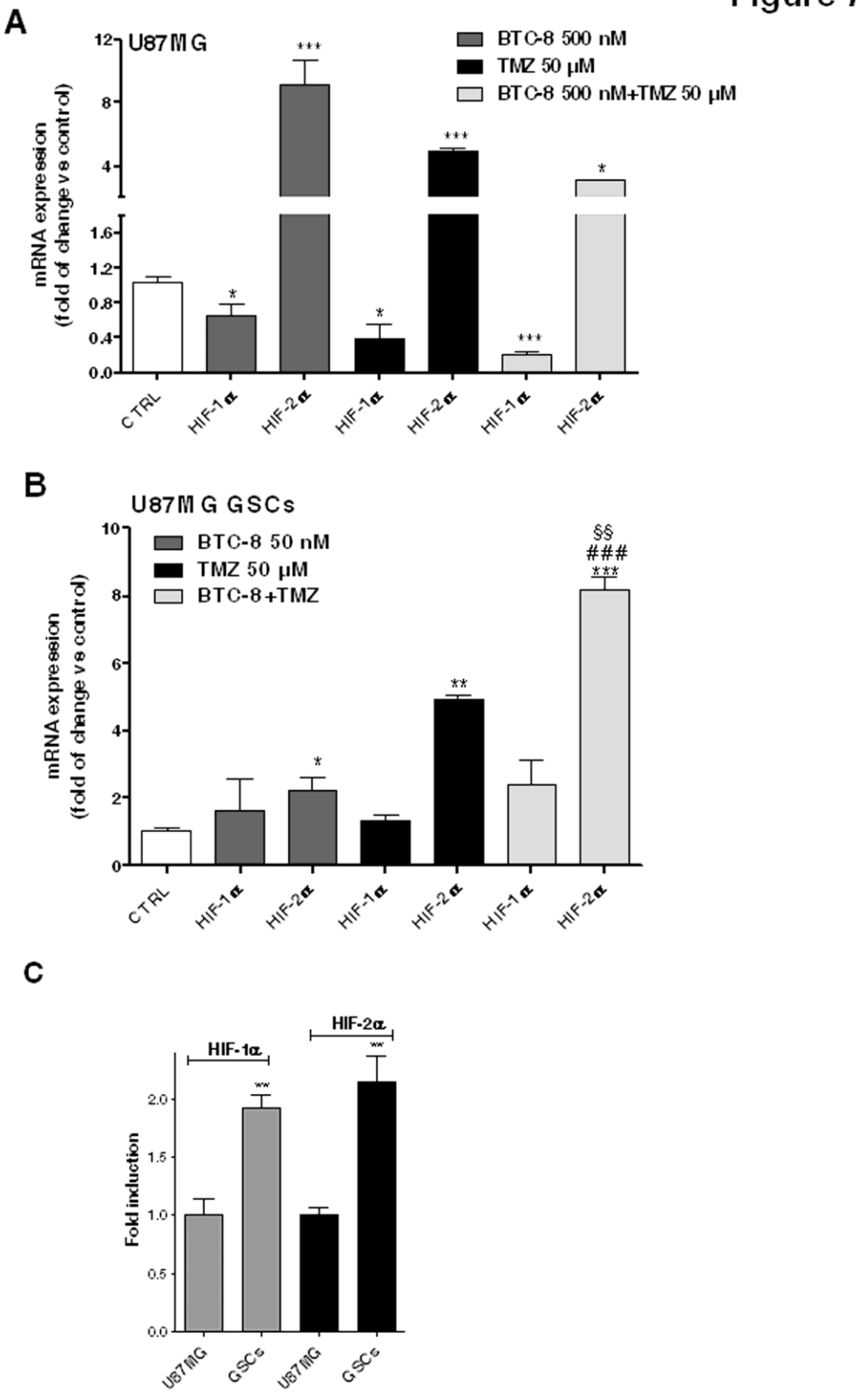
A
U87MG
BTC-8 500 nM
TMZ 50 µM
BTC-8 500 nM+TMZ 50 µM
mRNA expression
(fold of change vs control)
CTRL
HIF-1α
HIF-2α
B
U87MG GSCs
BTC-8 50 nM
TMZ 50 µM
BTC-8+TMZ
§§
###
C
HIF-1α
HIF-2α
Fold induction
U87MG
GSCs

Figure 8

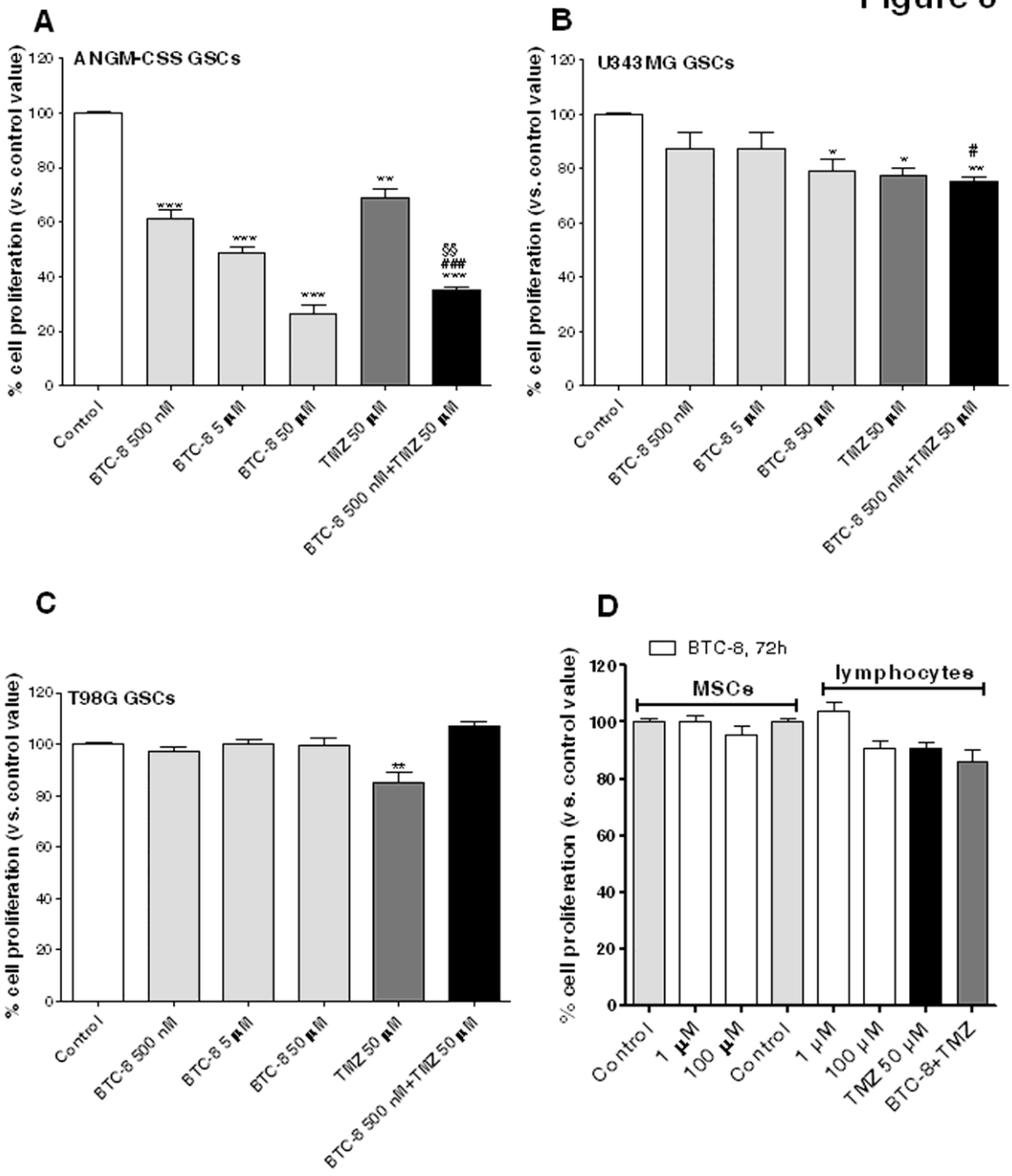
A
ANGM-CSS GSCs
% cell proliferation (vs. control value)
Control
BTC-8 500 nM
BTC-8 5 µM
BTC-8 50 µM
TMZ 50 µM
BTC-8 500 nM+TMZ 50 µM
B
U343MG GSCs
C
T98G GSCs
D
BTC-8, 72h
MSCs
lymphocytes
% cell proliferation (vs. control value)
1 µM
100 µM
TMZ 50 µM
BTC-8+TMZ

Figure Legends

Fig. 1. Effects of BTC-8 on U87MG cell proliferation. (**A**) U87MG cells were treated in complete medium with the indicated concentrations of BTC-8 or TMZ (50 μM) for 72 h. At the end of the treatment, cell proliferation was evaluated as described in the Methods section. The data are expressed as percentages relative to untreated cells (control), which were set at 100% (mean ± SEM; N = 3). (**B**) U87MG were transfected with a siRNA random (black bars) or a specific siRNA for Bax (white bars), and incubated with different BTC-8 concentrations (10 nM-50 μM) for 48 h. Following treatment, cell proliferation was evaluated with MTS assay, as described in the Methods Section. The data are expressed as a percentage with respect to that of untreated cells (control), which was set to 100% (mean values ± SEM, N = 3). (**C**) U87MG cells were treated in complete medium with BTC-8 (500 nM) and/or TMZ (50 μM) for 72 h. When indicated, cells were subsequently washed-out for additional 72 h in drug-free medium. Following treatment, cell proliferation was evaluated as described in the Methods section. The data are expressed as percentages relative to untreated cells (control), which were set at 100% (mean ± SEM; N = 3). (**D**) Isobolar analysis showing the interactions between BTC-8 and TMZ in U87MG cells treated for 72h. The IC_{50} values for TMZ and BTC-8 are shown on the X- and Y-axis, respectively. The theoretical $IC_{50,add}$ values are represented by open points on the additivity line. The $IC_{50,mix}$ values are represented by solid points (proportion of BTC-8 and TMZ that produced a 50% effect). The significance of the differences was determined by one-way ANOVA and Bonferroni's post hoc test: *P≤0.05, **P ≤ 0.01, ***P ≤ 0.001 vs. the control; #P ≤ 0.05, ##P ≤0.01, ### P ≤ 0.001 vs. the cells treated with BTC-8 for 72 h; §§ P ≤ 0.01, §§§ P ≤ 0.001 vs. the cells treated with TMZ for 72 h.

Fig. 2. Effects of BTC-8 on U87MG cell cycle, viability and Δψm. (**A**) U87MG cells were treated for 72 h in complete medium with DMSO as control and with the indicated concentrations of BTC-8 (10 nM-50 μM). At the end of the treatments, cell viability was measured using CellTrace dye labelling, as described in the Methods section. The data are expressed as number of live or dead cells (mean ± SEM, N=3). (**B**) U87MG cells were treated for 72 h with DMSO (control), BTC-8 (500 nM) and/or TMZ (50 μM). At the end of the treatment periods, the cells were collected and the level of phosphatidylserine externalisation was evaluated using the Annexin V-staining protocol. The data were expressed as the percentage of apoptotic cells versus the total number of cells (mean ± SEM; N = 3). (**C**) U87MG cells were treated for 72 h with DMSO (control), BTC-8 (500 nM) and TMZ (50 μM),

and the cell cycle was analyzed. The data were expressed as percentage of cell in the different phases (G0/G1, G2 or S) versus total cell number (mean ± SEM; N = 3). (**D)** Mithocondria, isolated from U87MG cells, were incubated for 15 min with BTC-8. Δψm (5 μg of proteins) was evaluated using JC-1 protocol. The data were expressed as the variation of JC-1 uptake into mitochondria, which was calculated as the difference between the RFU at the beginning and those read after 10 min (mean ± SEM; N = 3). (**E**) U87MG were treated for 72 h with DMSO (control), or BTC-8 (500 nM) and/or TMZ (50 μM). At the end of treatments, the mitochondria were isolated and Δψm was evaluated as in (C). (**E**) U87MG were treated for 72 h with DMSO (control), BTC-8 (500 nM) and/or TMZ (50 μM). At the end of treatments, the level of caspase 3/7 activation was evaluated as described in the Methods section. The data were expressed as the percentage of caspase positive cells versus the total number of cells, and are the mean ± SEM of three different experiments. *P ≤ 0.05, **P ≤ 0.01, ***P ≤ 0.001 vs. the control; §§ P ≤ 0.01, §§§ P ≤ 0.001 vs. the cells treated with TMZ for 72 h; # P ≤ 0.05, ### P ≤ 0.001 vs. the cells treated with BTC-8 for 72 h.

Fig. 3. Effects of BTC-8 and TMZ co-treatment on ANGM-CSS, T98G and U343MG cell proliferation. (**A**) ANGM-CSS (**B**) U343MG or (**C**) T98G cells were treated in complete medium with the indicated concentrations of BTC-8 (500 nM-50 μM), and/or TMZ (50 μM) for 72 h. At the end of treatment, cell proliferation was measured by MTS assay. The data are expressed as percentages relative to untreated cells (control), which were set at 100%, and represent the mean ± SEM of three independent experiments, each performed in triplicate. (**D, E**) The total RNA was extracted from U87MG cells (control), U343MG, T98G and ANGM-CSS cells. The relative mRNA quantification of the markers Bax, Bcl-2 and Bcl-XL (D) and the bax/Bcl-2 ratio (E) was performed by Real-time PCR, as described in the Methods section. The data were expressed as the fold change relative to the level of expression in U87MG cells, and they are the mean values ± SEM of two different experiments. The significance of the differences was determined by one-way ANOVA and Bonferroni's post hoc test: *P≤ 0.05, **P≤ 0.01, ***P ≤ 0.001 vs. the control; § P ≤ 0.05, §§§ P ≤ 0.001 vs. the cells treated with TMZ for 72 h; # P ≤ 0.05, ## P ≤ 0.01, ### P ≤ 0.001 vs. the cells treated with BTC-8 for 72 h.

Fig. 4. Effects of BTC-8 on U87MG-derived GSC proliferation. (**A**) GSCs isolated from U87MG were incubated with different concentrations of BTC-8 (0,1 nM-50 μM) for seven days. (**B)** U87MG and GSCs were collected and Bax mRNA was quantified by real time PCR analysis. (**C**) GSCs were treated in complete medium with BTC-8 (50 nM) and/or TMZ (50

μM) for seven days. When indicated, cells were subsequently washed-out for additional seven days in drug-free medium. At the end of treatment, cell proliferation was measured by MTS assay. ***P ≤ 0.001 vs. the control; §§ P ≤ 0.01, §§§ P ≤ 0.001 vs. the cells treated with TMZ for 72 h; ### P ≤ 0.001 vs. the cells treated with BTC-8 for 72 h.

Fig. 5. Effect of BTC-8 on the sphere-derived cell morphology and on the formation of U87MG-derived GSCs. (**A**) The GSCs were treated with complete NSC medium containing DMSO (control) or the indicated concentrations of BTC-8 and /or TMZ for 7 days. (**A**) Representative cell micrographs after 7 days of treatment were shown. (**B**) The number of the culture plates occupied by the spheres and (**C**) the area of neurospheres were scored after 7 days of treatment. The counts represent the mean values ± SEM of three independent experiments (**D**) U87MG were incubated with DMSO, BTC-8 and/or TMZ in a defined serum-free NSC medium for 9 days. Representative pictures of the cells after 9 days of incubation were shown. The mean diameter of the new formed spheres (**E**) and the number (**F**) were scored using the ImageJ program. The data represent the means ± SEM of three pictures from two independent experiments. *P≤0,05, ***P ≤ 0.001 vs. the control or DMSO. §§ P ≤ 0.01, §§§ P ≤ 0.001 vs. the cells treated with TMZ for 7 days; ##P≤0.05, ### P ≤ 0.001 vs. the cells treated with BTC-8 for 7 days.

Fig. 6. Effects of BTC-8 on U87MG-derived GSC cycle, viability and Δψm. (**A**) GSCs were treated for 72 h with DMSO (control), BTC-8 (50 nM) and TMZ (50 μM), and the cell cycle was analyzed. The data were expressed as percentage of cell in the different phases (G0/G1, G2 or S) versus total cell number (mean ± SEM; N = 3). (**B**) GSCs were treated for seven days as in (A). At the end of the treatment periods, the cells were collected and the level of phosphatidylserine externalisation was evaluated using the Annexin V-staining protocol. The data were expressed as the percentage of apoptotic cells versus the total number of cells, (mean ± SEM; N = 3). (**C**) GSCs were treated for seven days with DMSO (control), or BTC-8 (50 nM) and/or TMZ (50 μM). At the end of treatments, the mitochondria were isolated and the Δψm (5 μg of proteins) was evaluated using JC-1 protocol. The data were expressed as the variation of JC-1 uptake into mitochondria (mean ± SEM; N = 3). (**D**) The cells were treated as in (A). At the end of the treatment periods, the cells were collected and the level of caspase 3/7 activation was evaluated as described in the Methods section (mean ± SEM; N = 3). *P ≤ 0.05, **P ≤ 0.01, ***P ≤ 0.001 vs. the control; §§§ P ≤ 0.001 vs. the cells treated with TMZ

for 7 days; ### P ≤ 0.001 vs. the cells treated with BTC-8 for 7 days.

Fig. 7. Effects of BTC-8 on HIF-α modulation in U87MG cells and in U87MG-derived GSCs. (**A**) U87MG cells were treated with BTC-8 (500 nM) and TMZ (50 μM), alone or in combination. At the end of the treatment periods, real Time RT-PCR analysis of HIF-α was performed. The data were expressed as the fold change vs. the levels of the control, which were set to 1, and are the mean values ± SEM of three different experiments. The significance of the differences was determined by one-way ANOVA and Bonferroni's post hoc test: *P ≤ 0.05, ***P ≤ 0.001 vs. the control. (**B**) GSCs were treated with BTC-8 (50 nM) and/or TMZ (50 μM). Real Time RT-PCR analysis of HIF-α was performed. (**C**) Real time analysis of HIF-α was performed in U87MG cells and in U87MG-derived GSCs. *P≤ 0.05, **P ≤ 0.01, ***P ≤ 0.001 vs. the control; §§ P ≤ 0.01 vs. the cells treated with TMZ for 7 days; ### P ≤ 0.001 vs. the cells treated with BTC-8 for 7 days.

Fig. 8. Effects of BTC-8 on the proliferation of GSCs, isolated from different GBM cell lines, and of normal cells. (**A-C**) Neurospheres derived from ANGM-CSS (**A**), U343MG (**B**) or T98G (**C**) cells were incubated with the indicated concentrations of BTC-8 (500 nM-50 μM) or TMZ (50 μM), alone or in combination, for seven days. At the end of treatment, cell proliferation was evaluated as described in the Methods Section. The data are expressed as a percentage with respect to that of untreated cells (control), which was set to 100% (mean values ± SEM, N = 3). (**D)** Human MSCs or lymphocytes were treated with DMSO or the indicated concentrations of BTC-8 and/or TMZ for 72 h. Cell viability was determined by MTS assay.*P ≤ 0.05, **P ≤ 0.01, ***P ≤ 0.001 vs. control cells; §§ P ≤ 0.01 vs. the cells treated with TMZ for 7 days; # P ≤0.05, ### P ≤0.001 vs cells treated with BTC-8.

References

(1) Carlsson, S. K., Brothers, S. P., and Wahlestedt, C. (2014) Emerging treatment strategies for glioblastoma multiforme. *EMBO Mol. Med. 6*, 1359-70.

(2) Ostrom, Q. T., Gittleman, H., Farah, P., Ondracek, A., Chen, Y., Wolinsky, Y., Stroup, N. E., Kruchko, C., and Barnholtz-Sloan, J. S. (2013) CBTRUS statistical report: Primary brain and central nervous system tumors diagnosed in the United States in 2006-2010. *Neuro-oncology 15*, ii1-ii56.

(3) Yuan, X., Curtin, J., Xiong, Y., Liu, G., Waschsmann-Hogiu, S., Farkas, D. L., Black, K. L., and Yu, J. S. (2004) Isolation of cancer stem cells from adult glioblastoma multiforme. *Oncogene 23*, 9392 – 9400.

(4) Reya, T., Morrison, S. J., Clarke, M. F., and Weissman, I. L. (2001) Stem cells, cancer, and cancer stem cells. *Nature 414*, 105-11.

(5) Bryukhovetskiy, I., Manzhulo, I., Mischenko, P., Milkina, E., Dyuizen, I., Bryukhovetskiy, A., and Khotimchenko, Y. (2016) Cancer stem cells and microglia in the processes of glioblastoma multiforme invasive growth. *Oncol. Lett. 12*, 1721-1728.

(6) Daniele, S., Zappelli, E., Natali, L., Martini, C., and Trincavelli, M. L. (2014) Modulation of A1 and A2B adenosine receptor activity: a new strategy to sensitise glioblastoma stem cells to chemotherapy. *Cell Death Dis. 5*, e1539.

(7) Iqbal, A., Eckerdt, F., Bell, J., Nakano, I., Giles, F. J., Cheng, S. Y., Lulla, R. R., Goldman, S., and Platanias, L. C. (2016) Targeting of glioblastoma cell lines and glioma stem cells by combined PIM kinase and PI3K-p110α inhibition. *Oncotarget 7*, 33192-201.

(8) Bao, S., Wu, Q., McLendon, R. E., Hao, Y., Shi, Q., and Hjelmeland, A. B. (2006) Glioma stem cells promote radioresistance by preferential activation of the DNA damage response. *Nature 444,* 756–760.

(9) Beier, D., Schulz, J. B., and Beier, C. P. (2011) Chemoresistance of glioblastoma cancer stem cells–much more complex than expected. *Mol. Cancer 10*, 128–138.

(10) Happold, C., Roth, P., Wick, W., Schmidt, N., Florea, A. M., and Silginer, M. (2012) Distinct molecular mechanisms of acquired resistance to temozolomide in glioblastoma cells.

J. Neurochem. 122, 444–455.

(11) Chen, J., Li, Y., Yu, T. S., McKay, R. M., Burns, D. K., Kernie, S. G., and Parada, L. F. (2012) A restricted cell population propagates glioblastoma growth after chemotherapy. *Nature 488*, 522-6.

(12) Vidal, S. J., Rodriguez-Bravo, V., Galsky, M., Cordon-Cardo, C., and Domingo-Domenech, J. (2014) Targeting cancer stem cells to suppress acquired chemotherapy resistance. *Oncogene 33*, 4451-63.

(13) Martinou, J. C., and Youle, R. J. (2011) Mitochondria in apoptosis: Bcl-2 family members and mitochondrial dynamics. *Dev. Cell. 21*, 92-101.

(14) Du, H., Wolf, J., Schafer, B., Moldoveanu, T., Chipuk, J. E., and Kuwana, T. (2011) BH3 domains other than Bim and Bid can directly activate Bax/Bak. *J. Biol. Chem. 286*, 491-501.

(15) Ni Chonghaile, T., and Letai, A. (2008) Mimicking the BH3 domain to kill cancer cells. *Oncogene 27*, 149−157.

(16) Stornaiuolo, M., La Regina, G., Passacantilli, S., Grassia, G., Coluccia, A., La Pietra, V., Giustiniano, M., Cassese, H., Di Maro, S., Brancaccio, D., Taliani, S., Ialenti, A., Silvestri, R., Martini, C., Novellino, E., and Marinelli, L. (2015) Structure-based lead optimization and biological evaluation of BAX direct activators as novel potential anticancer agents. *J. Med. Chem. 58*, 2135-48.

(17) Williams, M. M., and Cook, R. S. (2015) Bcl-2 family proteins in breast development and cancer: could Mcl-1 targeting overcome therapeutic resistance? *Oncotarget 6*, 3519

(18) Cartron, P. F., Loussouarn, D., Campone, M., Martin, S. A., and Vallette, F. M. (2012) Prognostic impact of the expression/ phosphorylation of the BH3-only proteins of the BCL-2 family in glioblastoma multiforme. *Cell death & disease 3*, e421.

(19) Ichim, G., and Tait, S. W. (2016) A fate worse than death: apoptosis as an oncogenic process. *Nature Reviews Cancer 16*, 539–548.

(20) Guerra, E., Cimadamore, A., Simeone, P., Vacca, G., Lattanzio, R., Botti, G., Gatta, V., D'Aurora, M., Simionati, B., Piantelli, M., and Alberti, S. (2016) p53, cathepsin D, Bcl-2 are joint prognostic indicators of breast cancer metastatic spreading. *BMC Cancer 16*, 649.

(21) Ko, T. K., Chuah, C. T. H., Huang, J. W. J., Ng, K. P., and Ong, S. T. (2014) The BCL2 inhibitor ABT-199 significantly enhances imatinib-induced cell death in chronic myeloid leukemia progenitors. *Oncotarget 5*, 9033–9038.

(22) Foster, K. A., Jane, E. P., Premkumar, D. R., Morales, A., and Pollack, I. F. (2014) Co-administration of ABT-737 and SAHA induces apoptosis, mediated by Noxa upregulation, Bax activation and mitochondrial dysfunction in PTEN-intact malignant human glioma cell lines. *J Neurooncol*. *120*, 459-72

(23) Berghauser Pont, L. M., Spoor, J. K., Venkatesan, S., Swagemakers, S., Kloezeman, J. J., Dirven, C. M., van der Spek, P. J., Lamfers, M. L., and Leenstra, S. (2014) The Bcl-2 inhibitor Obatoclax overcomes resistance to histone deacetylase inhibitors SAHA and LBH589 as radiosensitizers in patient-derived glioblastoma stem-like cells. *Genes Cancer 5*, 445–459.

(24) Delbridge, A. R., and Strasser, A. (2015) The BCL-2 protein family, BH3-mimetics and cancer therapy. *Cell Death Differ. 22*, 1071-80.

(25) Gavathiotis, E., Suzuki, M., Davis, M. L., Pitter, K., Bird, G. H., Katz, S. G., Tu, H. C., Kim, H., Cheng, E. H., Tjandra, N., and Walensky, L. D. (2008) BAX activation is initiated at a novel interaction site. *Nature 455*, 1076-81.

(26) Gavathiotis, E., Reyna, D. E., Bellairs, J. A., Leshchiner, E. S., and Walensky, L. D. (2012) Direct and selective small-molecule activation of proapoptotic BAX. *Nat. Chem. Biol. 8*, 639-45.

(27) Zhao, G., Zhu, Y., Eno, C. O., Liu, Y., Deleeuw, L., Burlison, J. A., Chaires, J. B., Trent, J. O. and Li, C. (2014) Activation of the proapoptotic Bcl-2 protein Bax by a small molecule induces tumor cell apoptosis. *Mol. Cell. Biol. 34*, 1198–1207.

(28) Xin, M., Li, R., Xie, M., Park, D., Owonikoko, T. K., Sica, G. L., Corsino, P. E., Zhou, J., Ding, C., White, M. A., Magis, A. T., Ramalingam, S. S., Curran, W. J., Khuri, F. R., and Deng, X. (2014) Small-molecule Bax agonists for cancer therapy. *Nat. Commun. 5*, 4935.

(29) Cristofanon, S., and Fulda, S. (2012) ABT-737 promotes tBid mitochondrial accumulation to enhance TRAIL-induced apoptosis in glioblastoma cells. *Cell Death Dis. 3*, e432.

(30) Costa, B., Bendinelli, S., Gabelloni, P., Da Pozzo, E., Daniele, S., Scatena, F., Vanacore, R., Campiglia, P., Bertamino, A., Gomez-Monterrey, I., Sorriento, D., Del Giudice, C., Iaccarino, G.,

Novellino, E., and Martini, C. (2013) Human glioblastoma multiforme: p53 reactivation by a novel MDM2 inhibitor. *PLoS One 8*, e72281.

(31) Hetschko, H., Voss, V., Senft, C., Seifert, V., Prehn, J. H., and Kögel, D. (2008) BH3 mimetics reactivate autophagic cell death in anoxia-resistant malignant glioma cells. *Neoplasia 10*, 873-85.

(32) Yu, C., Friday, B. B., Yang, L., Atadja, P., Wigle, D., Sarkaria, J., and Adjei, A. A. (2008) Mitochondrial Bax translocation partially mediates synergistic cytotoxicity between histone deacetylase inhibitors and proteasome inhibitors in glioma cells. *Neuro Oncol. 10*, 309-19.

(33) Voss, V., Senft, C., Lang, V., Ronellenfitsch, M. W., Steinbach, J. P., Seifert, V., and Kögel, D. (2010) The pan-Bcl-2 inhibitor (-)-gossypol triggers autophagic cell death in malignant glioma. *Mol. Cancer Res. 8*, 1002-16.

(34) Tallarida, R. J., Stone, D. J. J. R., McCary, J. D., and Raffa, R. B. (1999) Response surface analysis of synergism between morphine and clonidine. *J. Pharmacol. Exp. Ther*. *289*, 8–13.

(35) Tallarida, R. J. (2002) The interaction index: a measure of drug synergism. *Pain 98*, 163–168.

(36) Kroemer, G., Galluzzi, L., and Brenner, C. (2007) Mitochondrial membrane permeabilization in cell death. *Physiol. Rev. 87*, 99-163.

(37) Luna-Vargas, M. P., and Chipuk, J. E. (2016) Physiological and Pharmacological Control of BAK, BAX, and Beyond. *Trends Cell Biol*. *26*, 906-917.

(38) Shi, L., Chen, J., Yang, J., Pan, T., Zhang, S., and Wang, Z. (2010) MiR-21 protected human glioblastoma U87MG cells from chemotherapeutic drug temozolomide induced apoptosis by decreasing Bax/Bcl-2 ratio and caspase-3 activity. *Brain Res. 1352*, 255-64.77

(39) Jiang, Z., Zheng, X., and Rich, K. M. (2003) Down-regulation of Bcl-2 and Bcl-xL expression with bispecific antisense treatment in glioblastoma cell lines induce cell death. *J. Neurochem. 84*, 273-81.

(40) Ishii, N., Maier, D., Merlo, A., Tada, M., Sawamura, Y., Diserens, A. C., and Van Meir, E. G. (1999) Frequent co-alterations of TP53, p16/CDKN2A, p14ARF, PTEN tumor suppressor genes in human glioma cell lines. *Brain Pathol. 9*, 469-79.

(41) Notarangelo, A., Trombetta, D., D'Angelo, V., Parrella, P., Palumbo, O., Storlazzi, C. T., Impera, L., Muscarella, L. A., La Torre, A., Affuso, A., Fazio, V. M., Carella, M., and Zelante, L. (2014) Establishment and genetic characterization of ANGM-CSS, a novel, immortal cell line derived from a human glioblastoma multiforme. *Int. J. Oncol. 44*, 717-24.

(42) Wang, C. C., Liao, Y. P., Mischel, P. S., Iwamoto, K. S., Cacalano, N. A., and McBride,

W. H. (2006) HDJ-2 as a target for radiosensitization of glioblastoma multiforme cells by the farnesyltransferase inhibitor R115777 and the role of the p53/p21 pathway. *Cancer Res*. *13*, 6756-62.

(43) Daniele, S., Sestito, S., Pietrobono, D., Giacomelli, C., Chiellini, G., Di Maio, D., Marinelli, L., Novellino, E., Martini, C., and Rapposelli, S. (2017) Dual inhibition of PDK1 and Aurora Kinase A: an effective strategy to induce differentiation and apoptosis of human glioblastoma multiforme stem cells. *ACS Chem. Neurosci. 8*, 100-114.

(44) Sestito, S., Nesi, G., Daniele, S., Martelli, A., Digiacomo, M., Borghini, A., Pietra, D., Calderone, V., Lapucci, A., Falasca, M., Parrella, P., Notarangelo, A., Breschi, M. C., Macchia, M., Martini, C., and Rapposelli, S. (2015) Design and synthesis of 2-oxindole based multi-targeted inhibitors of PDK1/Akt signaling pathway for the treatment of glioblastoma multiforme. *Eur. J. Med. Chem. 105*, 274-88.

(45) Gratas, C., Séry, Q., Rabé, M., Oliver, L., and Vallette, F. M. (2014) Bak and Mcl-1 are essential for Temozolomide induced cell death in human glioma. *Oncotarget 5*, 2428-35.

(46) Le Pen, J., Laurent, M., Sarosiek, K., Vuillier, C., Gautier, F., Montessuit, S., Martinou, J. C., Letaï, A., Braun, F., and Juin, P. P. (2016) Constitutive p53 heightens mitochondrial apoptotic priming and favors cell death induction by BH3 mimetic inhibitors of BCL-xL. *Cell Death Dis. 7*, e2083.

(47) Stegh, A. H., Brennan, C., Mahoney, J. A., Forloney, K. L., Jenq, H. T., Luciano, J. P., Protopopov, A., Chin, L., and Depinho, R. A. (2010) Glioma oncoprotein Bcl2L12 inhibits the p53 tumor suppressor. *Genes Dev. 24*, 2194-204.

(48) Zhou, Z., Meng, M., and Ni, H. (2017) Chemosensitizing effect of Astragalus Polysaccharides on nasopharyngeal carcinoma cells by inducing apoptosis and modulating expression of Bax/Bcl-2 Ratio and caspases. *Med. Sci. Monit. 23*, 462-469.

(49) Carotenuto, F., Coletti, D., Di Nardo, P., and Teodori, L. (2016) α-Linolenic Acid reduces TNF-induced apoptosis in C2C12 myoblasts by regulating expression of apoptotic proteins. *Eur. J. Transl. Myol*. *26*, 6033.

(50) Mohammadi, A., Yaghoobi, M. M., GholamhoseynianNajar, A., Kalantari-Khandani, B., Sharifi, H., and Saravani, M. (2016) HSP90 inhibitor enhances anti-proliferative and apoptotic effects of celecoxib on HT-29 colorectal cancer cells via increasing BAX/BCL-2 ratio. *Cell Mol. Biol. (Noisy-le-grand) 62*, 62-67.

(51) Masuelli, L., Benvenuto, M., Di Stefano, E., Mattera, R., Fantini, M., De Feudis, G., De Smaele, E., Tresoldi, I., Giganti, M. G., Modesti, A., and Bei, R. (2017) Curcumin blocks autophagy and activates apoptosis of malignant mesothelioma cell lines and increases the

survival of mice intraperitoneally transplanted with a malignant mesothelioma cell line. *Oncotarget* doi: 10.18632/oncotarget.14907.

(52) Kang, M. K., and Kang, S. K. (2007) Tumorigenesis of chemotherapeutic drug-resistant cancer stem-like cells in brain glioma. *Stem Cells Dev. 16*, 837-47.

(53) Daniele, S., Giacomelli, C., Zappelli, E., Granchi, C., Trincavelli, M. L., Minutolo, F., and Martini, C. (2015) Lactate dehydrogenase-A inhibition induces human glioblastoma multiforme stem cell differentiation and death. *Sci. Rep. 5*, 15556.

(54) Tagscherer, K. E., Fassl, A., Campos, B., Farhadi, M., Kraemer, A., Böck, B. C., Macher-Goeppinger, S., Radlwimmer, B., Wiestler, O. D., Herold-Mende, C., and Roth, W. (2008) Apoptosis-based treatment of glioblastomas with ABT-737, a novel small molecule inhibitor of Bcl-2 family proteins. *Oncogene 27*, 6646-56.

(55) Liu, G., Yuan, X., Zeng, Z., Tunici, P., Ng, H., Abdulkadir, I. R., Lu, L., Irvin, D., Black, K. L., and Yu, J. S. (2006) Analysis of gene expression and chemoresistance of CD133+ cancer stem cells in glioblastoma. *Mol. Cancer 5*, 67.

(56) Ma, X., Zhou, J., Zhang, C. X., Li, X. Y., Li, N., Ju, R. J., Shi, J. F., Sun, M. G., Zhao, W. Y., Mu, L. M., Yan, Y., and Lu, W. L. (2013) Modulation of drug-resistant membrane and apoptosis proteins of breast cancer stem cells by targeting berberine liposomes. *Biomaterials 34*, 4452-65.

(57) Wang, L., Guo, H., Yang, L., Dong, L., Lin, C., Zhang, J., Lin, P., and Wang, X. (2013) Morusin inhibits human cervical cancer stem cell growth and migration through attenuation of NF-κB activity and apoptosis induction. *Mol. Cell. Biochem. 379*, 7-18.

(58) Li, Z., Bao, S., Wu, Q., Wang, H., Eyler, C., Sathornsumetee, S., Shi, Q., Cao, Y., Lathia, J., McLendon, R. E., Hjelmeland, A. B., and Rich, J. N. (2009) Hypoxia-inducible factors regulate tumorigenic capacity of glioma stem cells. *Cancer Cell 15*, 501-13.

(59) Soeda, A., Park, M., Lee, D., Mintz, A., Androutsellis-Theotokis, A., McKay, R. D., Engh, J., Iwama, T., Kunisada, T., Kassam, A. B., Pollack, I. F., and Park, D. M. (2009) Hypoxia promotes expansion of the CD133-positive glioma stem cells through activation of HIF-1alpha. *Oncogene 28*, 3949-59.

(60) Méndez, O., Zavadil, J., Esencay, M., Lukyanov, Y., Santovasi, D., Wang, S. C., Newcomb, E. W., and Zagzag, D. (2010) Knock down of HIF-1alpha in glioma cells reduces migration in vitro and invasion in vivo and impairs their ability to form tumor spheres. *Mol. Cancer 9*, 133.

(61) Lou, F., Chen, X., Jalink, M., Zhu, Q., Ge, N., Zhao, S., Fang, X., Fan, Y., Björkholm, M., Liu, Z., and Xu, D. (2007) The opposing effect of hypoxia-inducible factor-2alpha on

expression of telomerase reverse transcriptase. *Mol. Cancer Res. 5*, 793-800.

(62) Zhou, Y., Zhou, Y., Shingu, T., Feng, L., Chen, Z., Ogasawara, M., Keating, M. J., Kondo, S., and Huang, P. (2011) Metabolic alterations in highly tumorigenic glioblastoma cells: preference for hypoxia and high dependency on glycolysis. *J. Biol. Chem. 286*, 32843-53.

(63) Ciavardelli, D., Rossi, C., Barcaroli, D., Volpe, S., Consalvo, A., Zucchelli, M., De Cola, A., Scavo, E., Carollo, R., D'Agostino, D., Forlì, F., D'Aguanno, S., Todaro, M., Stassi, G., Di Ilio, C., De Laurenzi, V., and Urbani, A. (2014) Breast cancer stem cells rely on fermentative glycolysis and are sensitive to 2-deoxyglucose treatment. *Cell Death Dis. 5*, e1336.

(64) Pietras, A., Hansford, L. M., Johnsson, A. S., Bridges, E., Sjölund, J., Gisselsson, D., Rehn, M., Beckman, S., Noguera, R., Navarro, S., Cammenga, J., Fredlund, E., Kaplan, D. R., and Påhlman, S. (2009) HIF-2alpha maintains an undifferentiated state in neural crest-like human neuroblastoma tumor-initiating cells. *Proc. Natl. Acad. Sci. U S A 106*, 16805-10.

(65) Hu, Y. Y., Fu, L. A., Li, S. Z., Chen, Y., Li, J. C., Han, J., Liang, L., Li, L., Ji, C. C., Zheng, M. H., and Han, H. (2014) Hif-1α and Hif-2α differentially regulate Notch signaling through competitive interaction with the intracellular domain of Notch receptors in glioma stem cells. *Cancer Lett. 349*, 67-76.

(66) Zheng, H., Ying, H., Yan, H., Kimmelman, A. C., Hiller, D. J., Chen, A. J., Perry, S. R., Tonon, G., Chu, G. C., Ding, Z., Stommel, J. M., Dunn, K. L., Wiedemeyer, R., You, M. J., Brennan, C., Wang, Y. A., Ligon, K. L., Wong, W. H., Chin, L., and DePinho, R. A. (2008) p53 and Pten control neural and glioma stem/progenitor cell renewal and differentiation. *Nature 455*, 1129-33.

(67) Simoni, E., Daniele, S., Bottegoni, G., Pizzirani, D., Trincavelli, M. L., Goldoni, L., Tarozzo, G., Reggiani, A., Martini, C., Piomelli, D., Melchiorre, C., Rosini, M., and Cavalli, A. (2012) Combining galantamine and memantine in multitargeted, new chemical entities potentially useful in Alzheimer's disease. *J. Med. Chem. 55*, 9708-21.

(68) Daniele, S., Taliani, S., Da Pozzo, E., Giacomelli, C., Costa, B., Trincavelli, M. L., Rossi, L., La Pietra, V., Barresi, E., Carotenuto, A., Limatola, A., Lamberti, A., Marinelli, L., Novellino, E., Da Settimo, F., and Martini, C. (2014) Apoptosis therapy in cancer: the firs Apoptosis therapy in cancer: the first single-molecule co-activating p53 and the translocator protein in glioblastoma. *Sci. Rep. 4*, 4749.